REVIEW

Check for updates

Advances in nanogenerator enabled smart mask-based self-powered health monitoring units

Mohamed A. Belal, [ID] [a] Swati Panda, [ID] [a] Udaykumar Khanapuram, [ID] *[b] Sugato Hajra, [ID] *[c] Kushal Ruthvik Kaja, [ID] [a] Rakesh Kumar Rajaboina, [ID] [b] Venkateswaran Vivekananthan, [ID] [d] Naratip Vittayakorn [ID] [e] and Hoe Joon Kim [ID] *[a]

The detection and analysis of volatile biomarkers in exhaled breath have emerged as promising non-invasive strategies for early disease diagnosis, therapeutic monitoring, and personalized healthcare. Traditional gas sensing platforms, however, often face limitations including dependency on external power sources, bulky designs, and inadequate sensitivity or selectivity under physiological conditions. This work provides a complete overview of recent improvements in self-powered gas sensors, with a special emphasis on their use in exhaled breath analysis for health monitoring. We begin by discussing the biomedical importance of breath-based diagnostics and the significant challenges associated with traditional sensor technology. Afterward, we investigate the mechanisms of energy harvesting systems such as triboelectric nanogenerators (TENGs) and piezoelectric nanogenerators (PENGs), which facilitate the self-powered operation without an external energy supply. Innovations in materials, structural design techniques, and integration strategies that improve mechanical flexibility, sensitivity, and gas selectivity are highlighted. We also highlight recent breakthroughs in wearable and portable gas sensing platforms that demonstrate real-time responsiveness and human-interfaced compatibility. Despite significant progress, challenges such as miniaturization, biomarker specificity, signal stability in dynamic environments, and large-scale manufacturability still need to be addressed. Finally, we discuss potential ways to address these barriers, envisioning a future where self-powered gas sensors play a transformative role in point-of-care diagnostics, continuous health monitoring, and smart healthcare ecosystems. This review aims to serve as a valuable resource for researchers and developers seeking to advance the field of self-powered biomedical sensing technologies.

1. Introduction

Gas sensor application in health monitoring is considered one of the non-invasive medical diagnostics, offering a painless and convenient method for early-stage disease detection.[1–3] For example, diabetes mellitus, characterized by the body's inability to metabolize glucose properly, has emerged as a global health crisis, leading to high blood sugar levels due to insufficient insulin or cellular resistance to insulin. This condition, responsible for

[a] *Department of Robotics and Mechatronics Engineering, Daegu Gyeongbuk Institute of Science & Technology (DGIST), Daegu, 42988, South Korea. E-mail: joonkim@dgist.ac.kr*

[b] *Department of Physics, National Institute of Technology, Warangal 506004, India. E-mail: kanapuram.udaykumar@nitw.ac.in*

[c] *Department of Electrical Engineering and Computer Science, Daegu Gyeongbuk Institute of Science & Technology (DGIST), Daegu, 42988, South Korea. E-mail: sugatohajra@dgist.ac.kr*

[d] *Center for Flexible Electronics, Department of Electronics and Communication Engineering, Koneru Lakshmaiah Education Foundation, Guntur, Andhra Pradesh, India*

[e] *Department of Chemistry, Faculty of Science, King Mongkut's Institute of Technology, Ladkrabang, Bangkok, Thailand*

6.7 million deaths and affecting 537 million adults worldwide, can cause severe complications such as heart disease, kidney failure, stroke, nerve damage, and vision loss.[4] To understand more about the detection of diseases, metabolomics is divided into targeted and untargeted approaches, where targeted analysis quantifies known metabolites using pure analytical standards, while untargeted analysis employs high-resolution mass spectrometry (HRMS) to detect both known and unknown compounds.[5] Furthermore, gas chromatography (GC) and HRMS remain the most accurate tools for analysing breath content. However, their cost, complexity, and the need for sample pre-treatment hinder their use in routine or on-the-go diagnostics.

To address the issue of the cost of the previous tools, smart real-time gas sensors are employed which can analyse human breath and give instantaneous results because the human breath contains a rich mixture of volatile organic compounds (VOCs).[6] With the developments in the gas sensor field, nowadays, the gas sensors can detect small concentrations of VOC biomarkers, which are metabolome compounds available at room temperature (RT), typically ranging from ppb to ppm, which are produced during cellular and biochemical reactions

within an organism.[5,7,8] Some specific biomarkers can be detected not only in exhaled breath, but also in saliva, tissues, urine, and blood, indicating specific diseases.[9–13] To extend more, acetone is a biomarker for diabetes, while ammonia and nitric oxide are biomarkers for kidney dysfunction and respiratory diseases, respectively, which are closely linked to underlying health conditions.[4,6,14,15] VOCs have been widely explored as non-invasive biomarkers integrated with microfluidics for diagnosing diseases such as cancer, with their levels correlating with cancer type, tumour characteristics, and treatment response. Specific VOCs like hexanal and heptanal serve as potential lung cancer markers, while changes in VOC profiles have also enabled the detection of infections like *Helicobacter*

pylori and conditions such as asthma and diabetes.[16–18] Therefore, the use of machine learning algorithms facilitates both quantitative and qualitative detection of mixed gases, addressing challenges such as interference signals and noise, and providing preliminary indications of potential disease types.[19]

Several researchers attempted to design a simple and cost-effective setup to detect the VOC gases using a conventional method, as more than 2000 VOCs, including alcohols, ketones, aldehydes, acids, terpenes, acetates, fatty acids, propionates, and sulfur-containing compounds, have been detected in exhaled breath and body fluids,[5,20,21] but they faced significant limitations when applying it to real-time health monitoring, particularly in wearable devices. The high-power consumption

Mohamed A. Belal

Mr. Mohamed A. Belal is a PhD candidate in the Robotics and Mechatronics Engineering Department, Daegu Gyeongbuk Institute of Science and Technology (DGIST), South Korea. He worked as a lab engineer and research assistant at the Egypt-Japan University of Science and Technology, Egypt from 2021 to 2024. He received a master's degree in organic chemistry from the Chemistry Department at Alexandria University (Egypt, 2019) and a BSc in Chemistry/Physics from the Faculty of Science at Damanhur University (Egypt, 2007–2011). His research interest focuses on gas sensors, supercapacitors, and inkjet printing technologies.

Swati Panda

Dr. Swati Panda is currently a Innocore Postdoctoral Fellow at Daegu Gyeongbuk Institute of Science and Technology (DGIST), South Korea. She graduated PhD from DGIST, South Korea, in 2025 from the Robotics and Mechatronics Engineering Department. She received her Bachelor's degree from Utkal University, Odisha, India, in 2018. She pursued her Master's degree from Siksha O Anusandhan University, India, with a specialization in Biotechnology in 2020. Her research interests focus on developing self-powered biosensors and biodegradable/biocompatible material-based piezoelectric/triboelectric energy harvesters.

Udaykumar Khanapuram

Dr. K. Uday Kumar received his M.Sc (Electronics and Instrumentation) degree from the University College of Science, Osmania University, India. He obtained his PhD degree in Physics from the Indian Institute of Technology Madras (IIT Madras), Chennai, in 2016. He is currently an Assistant Professor at the Department of Physics, National Institute of Technology Warangal, India. His research focuses on metal–organic frameworks, metal oxides, and 2D materials for different energy harvesting applications.

Sugato Hajra

Dr. Sugato Hajra is currently a postdoctoral researcher at Daegu Gyeongbuk Institute of Science and Technology (DGIST), South Korea. He received a Bachelor in Technology degree from Siksha O Anusandhan University, India, in 2017. He pursued his M.Tech. degree with a specialization in VLSI and Embedded Systems at Siksha O Anusandhan University, and also served as a joint researcher at the Advanced Multifunctional and Materials Laboratory in the Institute of Technical Education and Research, Bhubaneswar, India, in 2019. He received the PhD degree in Robotics and Mechatronics Engineering in 2024 from DGIST, South Korea. His research interests mainly include lead-free piezoelectric/multiferroic materials, metal–organic frameworks, solid-state electronic devices, and hybrid energy harvesters.

due to the operation temperature is a major hurdle, making these sensors impractical for long-term use. Additionally, many traditional sensors struggle with achieving the high sensitivity needed to detect trace levels of biomarkers, and they often lack the responsiveness required for real-time data capture under dynamic conditions. These challenges have driven the development of self-powered gas sensors, which offer a transformative solution for next-generation healthcare systems. Designed to be operated without external power sources, these sensors leverage energy harvesting mechanisms such as piezoelectric and triboelectric technologies. By converting mechanical energy into electricity, self-powered sensors enable continuous and low-maintenance operation. This energy autonomy, combined with miniaturization and integration potential, makes

them ideal for wearable and portable devices aimed at real-time, personalized health monitoring.

Technological progress has expanded the horizons for these devices. Self-powered gas sensors are now powered by nanogenerators, photothermal energy, and enzyme-based biofuel cells to convert energy and detect target gases efficiently.[22–25] Advanced materials, such as molybdenum disulfide (MoS_2), ZnO nanostructures, metal–organic frameworks (MOFs), and graphene hybrids, offer high surface areas, tunable properties, and dual functionality for sensing and energy harvesting.[9,26,27] For example, Tung et al.[28] developed hybrid materials of graphene with MOFs such as ZIF-8, UiO-66, and CuBTC to detect different biomarkers such as methanol, ethanol, chloroform, acetone, acetonitrile, and tetrahydrofuran (THF). The graphene/CuBTC

Mr. Kushal Ruthvik Kaja is currently a doctoral student at the Daegu Gyeongbuk Institute of Science and Technology. He received a Bachelor's degree from Andhra Loyola College, India, in 2021. He received his Master's in Physics from VIT-AP University, India, in 2023. His research interests focus on solid–solid, solid–liquid and waste-based triboelectric energy harvesters.

Kushal Ruthvik Kaja

Dr. R. Rakesh Kumar received his PhD from the Department of Instrumentation and Applied Physics, Indian Institute of Science Bangalore, India. He worked as visiting faculty at the Department of Physics, IISER-Bhopal, in 2015. He is currently an Assistant Professor at the National Institute of Technology (NIT) Warangal, in the Dept. of. Physics from 2018 onwards. His research interests are piezo and triboelectric nanogenerators, 2D materials, waste-to-energy, and self-powered sensors.

Rakesh Kumar Rajaboina

Dr. Venkateswaran Vivekananthan is currently an Associate Professor in the Centre for Flexible Electronics, Department of Electronics and Communication Engineering, KL University, India. Also, he is the Co-Coordinator for the DST-PURSE sponsored research activity in the KL University. He has worked as a Research Associate in the University of Surrey, United Kingdom, and as a Post-doctoral Researcher at Jeju National University, South Korea. He obtained his PhD degree in Applied Energy Systems with major in Mechatronics Engineering from Jeju National University, South Korea. He has also received the Presidential Research Excellence Award for outstanding research during his PhD. His research focuses primarily on energy harvesting using triboelectric, piezoelectric, and hybrid nanogenerators with the combination of inorganic and biopolymer materials for self-powered nanosystems.

Venkateswaran Vivekananthan

Dr. Naratip Vittayakorn is a Professor of Materials Science and the Director of Advanced Materials Research (AMR) at King Mongkut's Institute of Technology Ladkrabang (KMITL) in Thailand. He earned his doctoral degree from Chiang Mai University, Thailand, and furthered his expertise as a visiting scientist at Iowa State University. With his impressive academic career, he has authored over 300 scholarly publications and holds 5 patents. His contributions to the fields of electroceramics, piezoelectricity, triboelectric nanogenerators, and the advancement of energy harvesting technology are noteworthy.

Naratip Vittayakorn

composite was highly sensitive and selective towards chloroform and methanol at low levels of 2.82 to 22.6 ppm. Moreover, Bayona et al.[16] developed a system for early-stage tumor detection by using a microfluidic device that mimics the ischemic conditions of solid tumors, providing valuable insights into the role of VOCs in this area. When embedded into wireless and IoT-based platforms, these sensors can deliver real-time data to healthcare providers, opening the door to point-of-care testing (POC) and remote diagnostics.[29]

Non-invasive VOC detection can be applied across various fields, extending beyond health monitoring and disease diagnosis to include areas such as environmental monitoring, food quality control, studying the last universal common ancestor (LUCA), and industrial process management.[30] For example, Maginga et al.[31] analyzed data from the implemented IoT technology in their experiment, successfully achieving nonvisual detection of northern leaf blight (NLB) in maize within four days post-inoculation by monitoring VOCs and ultrasound emissions. Despite their promising potential, self-powered gas sensors still face several challenges that have to be addressed for successful deployment in real-world medical applications. Achieving high sensitivity and selectivity remains a key obstacle, especially when detecting trace biomarkers in complex and variable environments such as human breath, because of the high operating temperature needed to activate the sensor to interact with the gas. However, in some materials, such as graphene, the interaction occurs using van der Waals forces, which indicates low sensitivity and selectivity.[29] Generally, the stability over long-term use is another concern, as sensor performance can degrade due to humidity, temperature fluctuations, or contamination.[32]

Moreover, the long recovery time and memory effect are considered a challenge, especially in the MOF, because of the pores and MOF–VOC interaction energy.[29] Miniaturizing these sensors while preserving performance is essential for their integration into wearable electronics. This will pave the way for reliable, continuous, and personalized health monitoring in early disease detection. For example, Chen et al.[33] integrated the wearable mask-inspired self-healing sensor array (MISSA) with artificial intelligence (AI) for long-term daily VOCs monitoring and assessment for personal health monitoring scenarios. Recent approaches for analysing sensor responses often apply different methods such as principal component analysis (PCA), linear discriminant analysis (LDA), and support vector machines (SVMs). These techniques are especially useful for managing large volumes of data and providing clear, actionable insights. Many sensor arrays use these analytical tools to detect and distinguish gases in their surrounding environment.[34]

TENGs generate static charges through friction between two polymer films with different electron affinities, each coated with metal electrodes.[35,36] TENGs operate in four distinct modes, namely, vertical contact-separation, lateral sliding, single-electrode, and freestanding triboelectric layer, each tailored to specific sensing applications. The vertical mode combines a simple structure with high instantaneous power density, stability, ease of design, and efficiency, making it well-suited for robust energy conversion. The lateral sliding mode generates a potential difference through horizontal motion, yielding high electrical output and adaptability for dynamic sensing. The single-electrode mode offers simplified system design and can function in either contact-separation or sliding configurations, though its output is relatively low. In contrast, the freestanding mode relies on asymmetric charge distribution between unconnected electrodes separated by a small gap, providing greater flexibility and enhanced signal strength.[37] These modes collectively allow TENG-based gas sensors to be lightweight, low-cost, sensitive, and adaptable to diverse environments.[38] Their output depends on triboelectric charge density, which is influenced by surface chemistry and environmental factors. Gas adsorption modifies surface resistivity through charge interactions, enabling self-powered sensing.[39,40]

In this review, we provide a comprehensive overview of recent advances in self-powered gas sensors, with a particular focus on their application in exhaled breath analysis for health monitoring. We highlight the importance of gas sensing in biomedical diagnostics and discuss the limitations of conventional sensor technologies, as shown in Fig. 1. The review then explores the growing demand for wearable and portable diagnostic tools, emphasizing the advantages of self-powered sensors and the energy harvesting mechanisms that enable their autonomous operation. Finally, this review addresses the current challenges such as sensitivity, selectivity, and miniaturization, and discusses the future prospects of self-powered gas sensors for achieving real-time, non-invasive, and personalized healthcare solutions.

Dr. Hoe Joon Kim is currently an Associate Professor in Robotics Engineering with the Daegu Gyeongbuk Institute of Science and Technology (DGIST), Daegu, South Korea, and also holds a courtesy appointment in the Information and Communication Engineering Department at DGIST. He received the BS degree from Johns Hopkins University, Baltimore, MD, USA, in 2009, and the MS and PhD degrees from the University of Illinois at Urbana–Champaign, Urbana, IL, USA, in 2011 and 2015, respec-

Hoe Joon Kim

tively, all in mechanical engineering. His research interests focus on piezoelectric MEMS resonators for RF wireless communication, nanogenerators, chemical/physical sensing, environmental monitoring, and emerging nanomaterials.
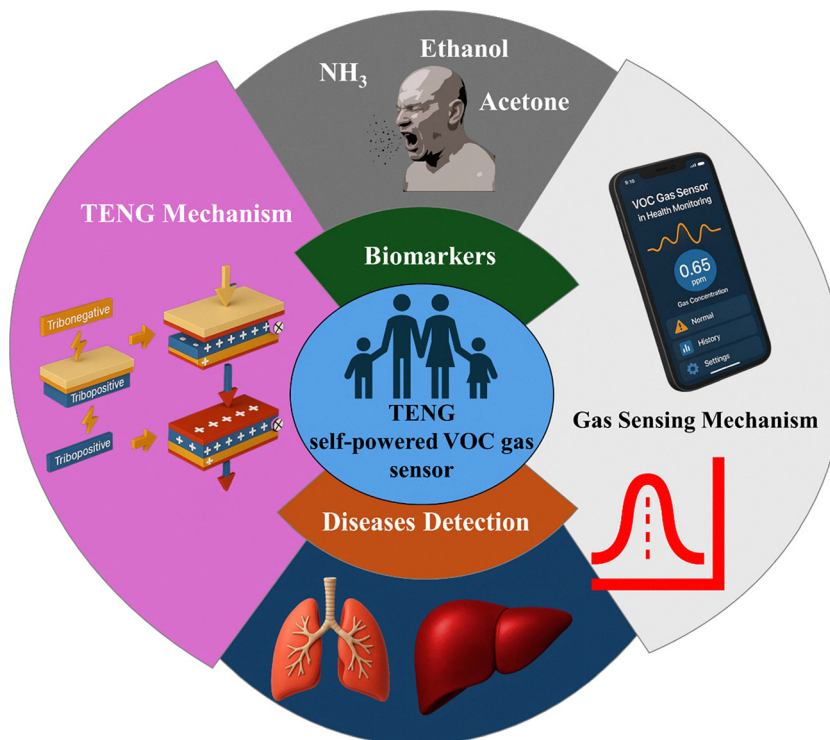
2. Working mechanism of piezoelectric and triboelectric nanogenerators

When PENGs are subjected to mechanical force, such as bending or pressing, the internal structure of the piezoelectric material becomes distorted. This distortion shifts the positions

Fig. 1 Schematic diagram representing the application of TENGs in the detection of some gases as biomarkers indicating diseases.

of positive and negative charge centres within the crystal lattice, resulting in polarization and the creation of an electric field inside the material, as shown in Fig. 2(i). The generated electric potential drives electrons through an external circuit, producing electrical energy. Once the force is released, the material returns to its original state, causing the charges to flow back and generating an alternating current. This cycle of mechanical deformation and relaxation enables the PENG to continually convert mechanical energy into electricity. PENGs generate electrical energy by converting mechanical stress in piezoelectric materials into usable power, enabling self-powered gas sensing. Gas concentrations are detected through variations in the potential difference. The intrinsic reactivity of piezoelectric materials, tuned by factors such as surface chemistry, grain size, and porous microstructure, enhances sensitivity and selectivity by facilitating interactions with target gases, producing measurable voltage changes that directly correspond with gas concentration.[41,42]

TENGs operate based on two fundamental physical effects: contact electrification (triboelectric effect) and electrostatic induction. There are four principal working modes, such as (a) contact separation (CS), (b) lateral sliding (LS), (c) single electrode (SE), and (d) free-standing mode, as shown in Fig. 2(ii). In CS mode, two materials with differing electron affinities come into contact and then separate, leading to electrons transfer between their surfaces. Upon separation, a potential difference arises, causing electrons to flow between electrodes to balance the charges, thus generating electricity. On the other hand, the LS mode involves two materials sliding

against each other laterally, generating surface charges through friction. The continuously changing contact area creates a varying potential, driving current through an external circuit. In the SE mode, one electrode is connected to the external load, while the another electrode is grounded. As the triboelectric layer moves relative to the electrode, it induces an electric field and a potential difference, prompting electron flow. In the free-standing mode, a charged triboelectric layer moves freely between two fixed electrodes. Its movement alters the electric field distribution, inducing a potential difference that drives electrons through the circuit.

3. TENG-based gas sensors

3.1. Alcohol sensing

TENGs have emerged as a promising solution for self-powered gas sensing. They enable the detection of critical biomarkers such as ethanol, acetone, and ammonia without external power sources.[24] The integration of TENGs with advanced sensing materials enhances sensitivity, selectivity, and real-time monitoring capabilities. In a notable study by Wen *et al.*,[43] a novel sensing mechanism was introduced through the fabrication of a blow-driven triboelectric nanogenerator (BD-TENG), as shown in Fig. 3.

This innovative device utilized electricity generated from human breath to produce a voltage output that directly correlates with the concentration of exhaled alcohol, regardless of variations in the airflow rate or blowing force. Acting as a
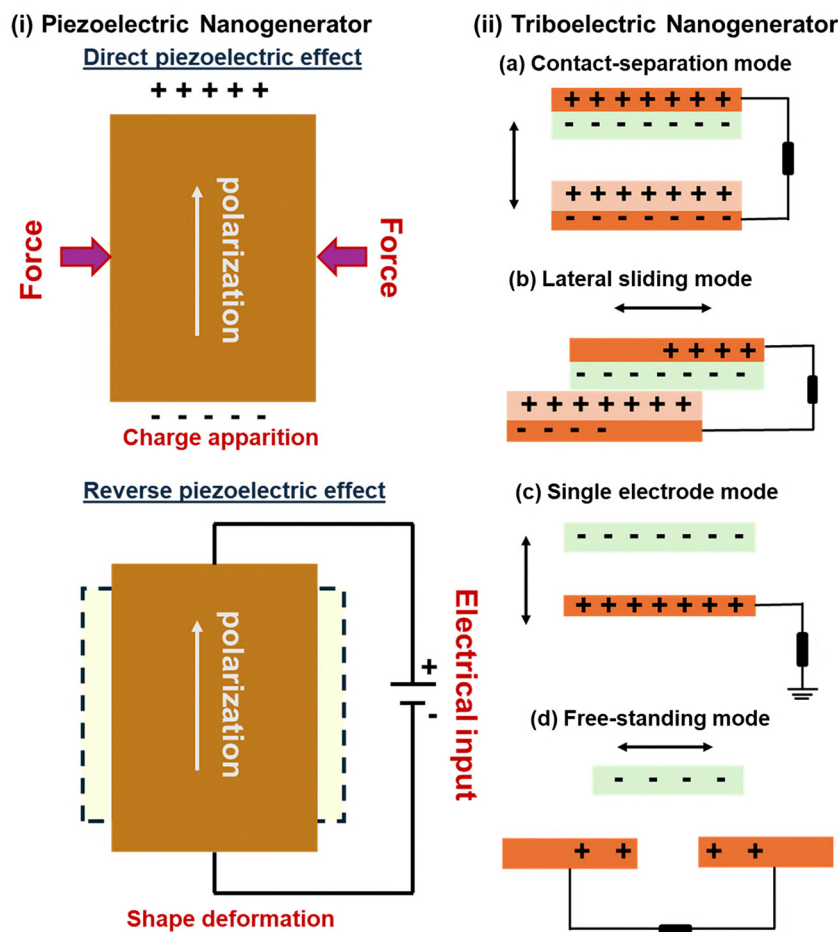
Fig. 2   (i) and (ii) Working mechanism of piezoelectric and triboelectric nanogenerators.

self-powered breathalyzer, the BD-TENG achieves a high response of 34 under optimal operational settings, with a response and recovery time of 11 and 20 s. The sensor also exhibits remarkable selectivity and resistance to interference in alcohol detection. Constructed from widely available polymer materials, the system remains lightweight and economical. This advancement not only introduces a fresh direction for gas sensing technologies but also broadens the functional landscape of TENGs in active, self-sustaining sensor applications.

To extend towards more applications related to health monitoring, breathing is a core physiological activity that offers valuable insights into an individual's health, serving as a reliable biomarker for both normal physiological function and disease conditions. Moreover, analyzing exhaled breath has emerged as a non-invasive, fast, and affordable technique for diagnosing and tracking various medical conditions by monitoring specific biomarker concentrations. In this context, Mohamadbeigi et al.[25] designed a self-sustaining ethanol breath sensor based on electrospun polyethylene oxide/copper(I) oxide composite nanofibers (PCNFs), as shown in Fig. 4. By operating within a simulated breath environment, this sensor detects ethanol concentrations ranging from 1 to 200 ppm. It is powered by an integrated contact-separation mode TENG,

eliminating the need for external power sources. The sensor demonstrates excellent sensitivity, with response values of 0.9 and 3.2 at 5 and 200 ppm of ethanol, respectively, even under high humidity (90% RH) and in the presence of interfering gases. Remarkably, it shows strong selectivity toward ethanol, with selectivity ratios of 10:1 over methanol and 25:1 over acetone. Additionally, it features fast response and recovery times of 2.7 and 5.8 s, respectively, for 200 ppm of ethanol at 90% RH. The stable and consistent performance of this PCNFs-based sensor under realistic conditions makes it a promising candidate for integration into wearable healthcare systems, enabling continuous monitoring of respiratory biomarkers and supporting real-time assessment of alcohol consumption compliance.

For self-powered and non-invasive diabetes diagnostics, enhancing the acetone-sensing performance and humidity resistance of TENGs represents a forward-looking approach. In a recent study, Liu et al.[44] introduced a novel TENG-based acetone sensor (CTS/ZnO–TAS) fabricated using a bilayer film composed of chitosan (CTS) and zinc oxide (ZnO), serving dual roles as both triboelectric and sensing layers (Fig. 5). This device exhibits a remarkable sensitivity of 1.95% per ppm and a high response of 19.02% toward 10 ppm of acetone, with
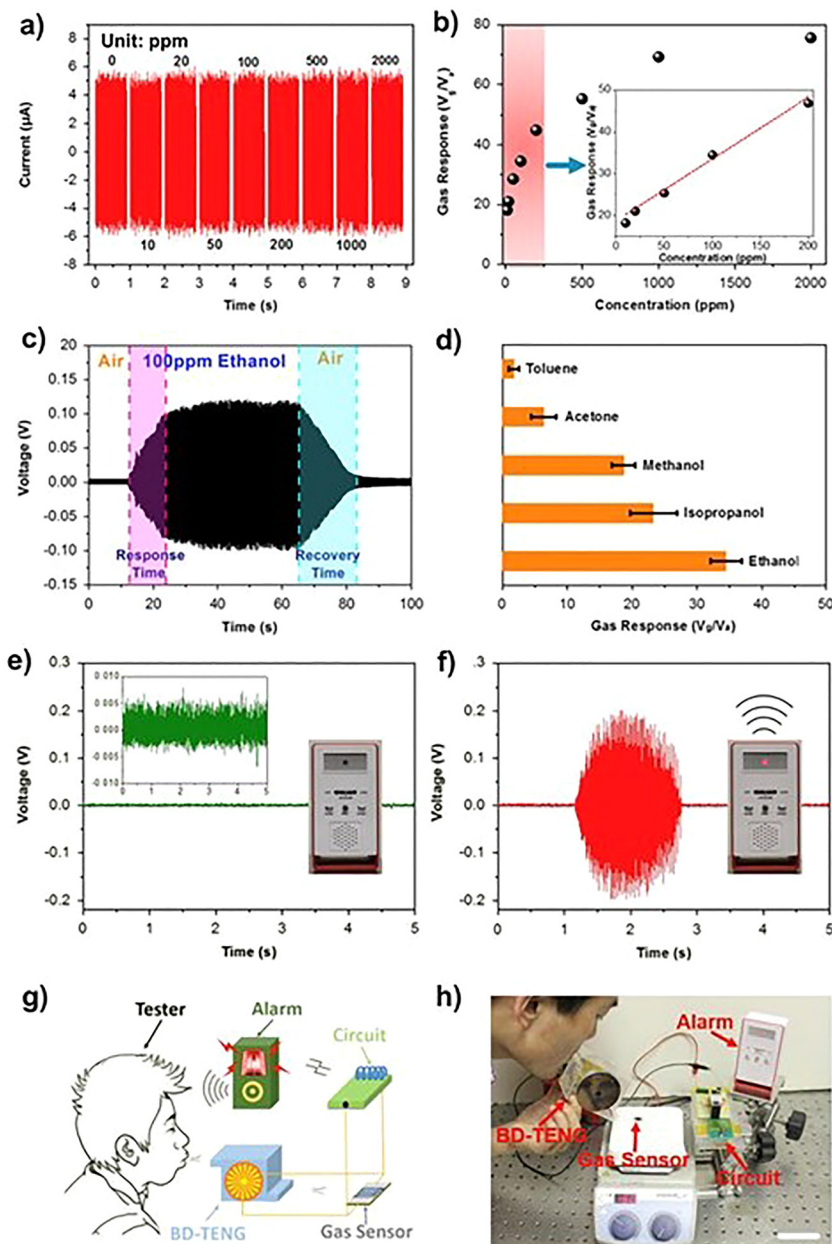
Fig. 3 (a) Under a fixed temperature of 160 °C, the variation of current with alcohol concentrations ranging from 10 to 2000 ppm. (b) The measured gas response curve in terms of output voltage; the inset is an enlarged view of the response curve in the range of 10 to 200 ppm. (c) A real-time, continuously measured voltage profile to show the dynamic response of the BD-TENG to ambient alcohol concentrations. (d) Test of the selectivity of the BD-TENG-based self-powered alcohol sensor. Demonstration of the BD-TENG as a self-powered breath analyzer. The acquired voltage signals of the BD-TENG when it was blown by a tester (e) before and (f) after drinking alcohol. The insets show that a wireless alarm was triggered with the siren on after drinking alcohol. (g) A schematic illustration and (h) a photograph showing the BD-TENG acting as a self-powered breath analyzer. The scale bar is 5 cm. (Reprinted with permission,[43] Copyright 2020, Elsevier.)

a limit of detection (LOD) as low as 1 ppm, even under high humidity conditions of 89.3% RH, outperforming the pure CTS. One of the reasons for the improved performance is the enhanced tolerance to moisture, which is primarily due to hydrogen bonding interactions between CTS and ZnO that effectively block hydrophilic groups and limit water uptake. In addition, the study proposes a synergistic sensing mechanism that combines triboelectric generation with gas-sensing

principles to explain the improved detection performance. Overall, the CTS/ZnO-based TENG platform demonstrates high humidity resistance and acetone sensitivity at RT, highlighting its potential for next-generation wearable breath sensors for early diabetes monitoring.

The high humidity in exhaled breath presents a significant challenge to the sensitivity and stability of wearable bioelectronic breath analysers. Inspired by the natural expansion and
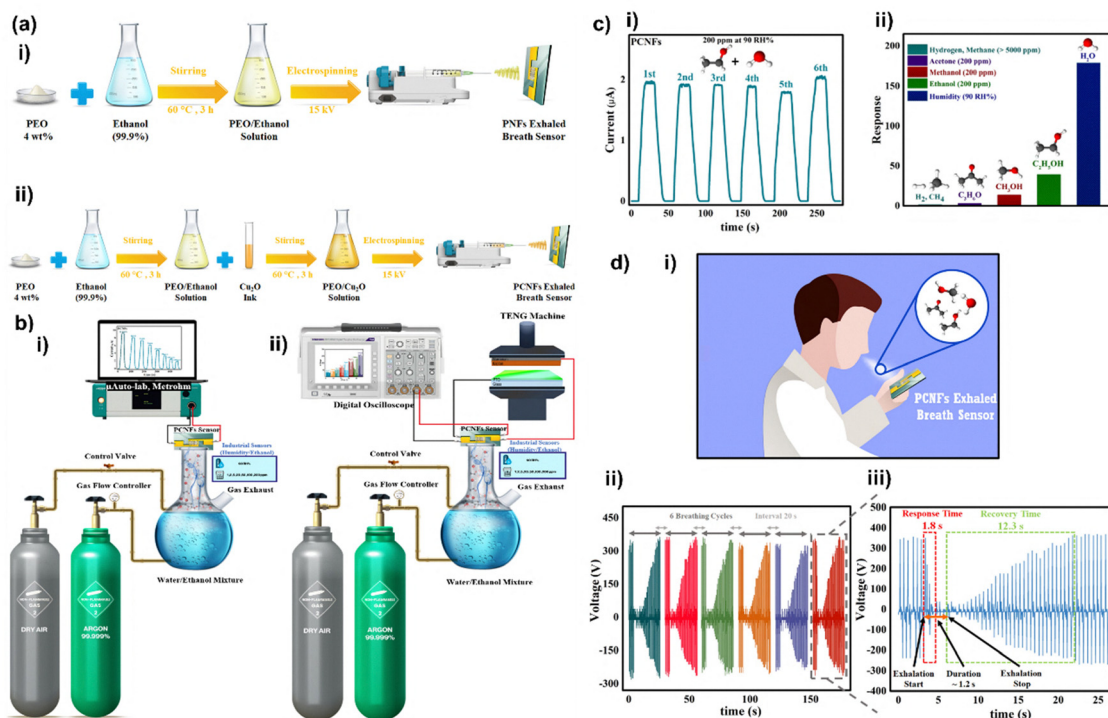
Fig. 4 (a) Synthesis procedures of exhaled breath sensors: (i) polyethylene oxide nanofiber (PNFs) sensor and (ii) polyethylene oxide/copper(I) oxide composite nanofibers (PCNFs) sensor. (b) The experimental set-up comprises an exhaled breath simulator intended to evaluate the performance of PCNFs sensors in various environments containing different ethanol concentrations (1, 2, 5, 20, 50, 100, 200 ppm) at 90 RH% through two distinct modes: (i) employing an external power source *via* a μAuto-lab system and (ii) utilizing a triboelectric nanogenerator for self-powering. (c) (i) Repeatability of the PCNFs sensor response to 200 ppm ethanol at 90 RH% for 6 repetitions; (ii) selectivity of the PCNFs sensor against ethanol, methanol, acetone, hydrogen, methane, carbon monoxide, and moisture. (d) (i) Schematic of a natural human breath test, (ii) the change in the output voltage of the PCNFs sensor when exposed to natural human breath, and (iii) the response and recovery time of the PCNFs sensor to natural human breath. (Reprinted with permission,[25] Copyright 2024, Springer Nature.)

contraction of pulmonary sections during breathing, Liu *et al.*[45] developed a respiration-driven triboelectric sensor (RTS) designed for dual functions: tracking respiratory biomechanics and detecting acetone in exhaled air. This was achieved by incorporating a tin oxide-doped polyethyleneimine membrane that acts as both the triboelectric and sensing component (Fig. 5). The RTS demonstrated excellent capability in monitoring respiratory parameters, effectively capturing airflow rates between 2 and 8 L min^{-1} and breathing frequencies ranging from 0.33 to 0.8 Hz. Additionally, it maintained high acetone sensitivity in the 2–10 ppm range, even under humid conditions. Finite element analysis simulations further supported the performance of the system. This innovative design presents a real-time, self-powered platform for respiratory and biochemical sensing, underscoring the effectiveness of the triboelectric–chemisorption hybrid mechanism and offering a promising avenue for future wearable breath analysis devices.

3.2. Ammonia (NH$_3$) gas sensing

Breathing is important in health monitoring, serving as a vital physiological function that not only reflects essential health indicators and aids in disease diagnosis but also offers a sustainable energy source for powering TENGs. The development of a simple, respiration-driven TENG for real-time, self-powered

respiratory monitoring is highly valuable for health assessments. For example, Wang *et al.*[46] developed a TENG based on a cerium-doped ZnO–polyaniline (PANI) nanocomposite film, capable of harvesting respiratory airflow energy and simultaneously detecting low concentrations of NH$_3$, airflow rate, and breathing patterns (Fig. 6). The fabricated device demonstrated impressive performance in monitoring respiratory flows ranging from 2 to 6 L min^{-1}, accurately identifying breathing frequencies, and distinguishing different breathing behaviours. Additionally, the sensor showed a steady decline in output voltage as the NH$_3$ concentration increased from 0.1 to 25 ppm, with high sensitivity toward trace-level NH$_3$ (0.1 to 1 ppm). These features highlight its potential for non-invasive, self-powered disease testing, especially in detecting exhaled NH$_3$ linked to kidney and liver dysfunctions. Overall, this work presents a simple yet effective strategy for building multifunctional respiratory monitoring systems powered only by human breath, advancing the field of wearable health diagnostics.

Exhaled breath analysis is a critical tool for the early, non-invasive diagnosis of various diseases. However, achieving reliable breath sensing remains challenging due to the poor selectivity of conventional gas sensors and the high humidity levels typically present in human breath. Addressing these challenges, Zhao *et al.*[7] utilized the processes of adsorption,
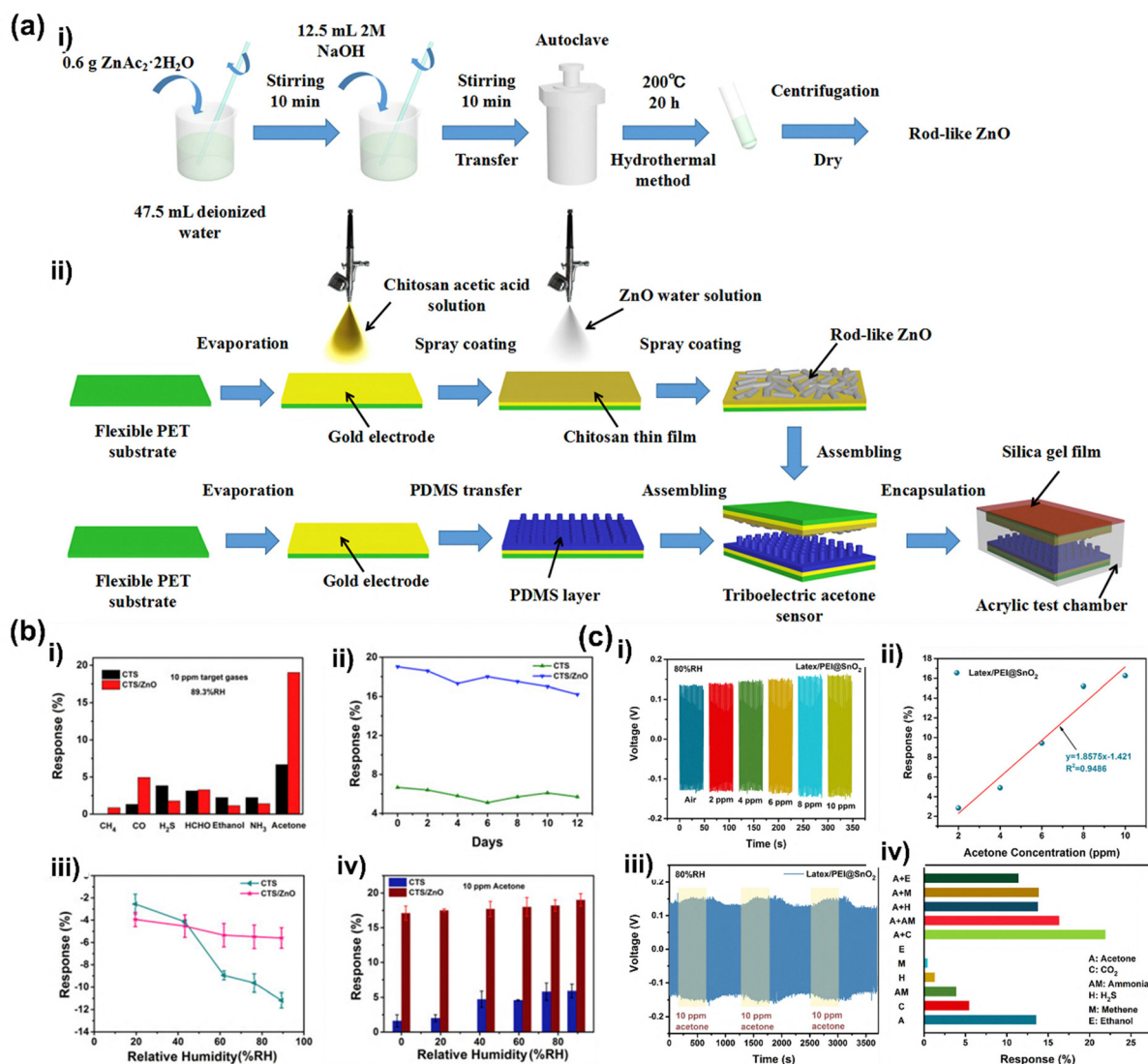
Fig. 5 (a) Schematic illustration of (i) the preparation of the ZnO and (ii) the fabrication of the TAS. (b) (i) Selectivity of the CTS/ZnO and CTS based TAS under 89.3% RH; (ii) long-term stability of CTS/ZnO–TAS and CTS–TAS; (iii) effect of different relative humidity levels on the responses of the CTS and CTS/ZnO based TAS; (iv) effect of different relative humidity levels on the sensing properties of 10 ppm of acetone by CTS/ZnO–TAS and CTS–TAS. (Reprinted with permission,[44] Copyright 2020, Elsevier.) (c) The acetone sensing performance of the RTS driven by a simulated respiration system. (i) Voltage outputs of the RTS with increasing concentration of acetone from 2 to 10 ppm under 80% RH; (ii) linear relationships between the acetone concentration and the response of the RTS. (iii) Cycle responses of the RTS toward 10 ppm of acetone. (iv) Cross-selectivity of the RTS toward different biomarkers. (Reprinted with permission,[45] Copyright 2022, ACS.)

dissolution, ionization, and migration of ammonia within wet, nonconjugated hydrophilic polymers to enable highly efficient ammonia detection, effectively turning humidity from a challenge into an advantage for enhancing sensor performance. Sensors based on nonconjugated polymers showed remarkable selectivity, successfully differentiating ammonia from other gases owing to its high solubility and strong ionization behaviour. Among these, a sensor made from polyvinylpyrrolidone (PVP) achieved an exceptional LOD of 0.5 ppm along with excellent selectivity. The underlying sensing mechanism was systematically explored using complex impedance plots (CIPs) and quartz crystal microbalance (QCM) analyses, offering deep insight into its operation. Furthermore, the effectiveness of the PVP-based sensor was validated under simulated breath conditions, highlighting its strong potential for practical, non-invasive medical diagnostic.

The detection of trace amounts of ammonia (NH_3) in exhaled breath is challenged by the high humidity and complex composition of human breath, which compromise selectivity and stability. Carboxyl-functionalized hydrogels can be activated by moisture to deliver high response and excellent selectivity toward NH_3; however, the high reactivity of carboxyl groups often compromises their chemical stability during sensing. To overcome this, Liu et al.[47] incorporated organic acids into a crosslinked polyethylene glycol diacrylate (PEGDA) hydrogel using thiol–ene photochemical reactions, creating
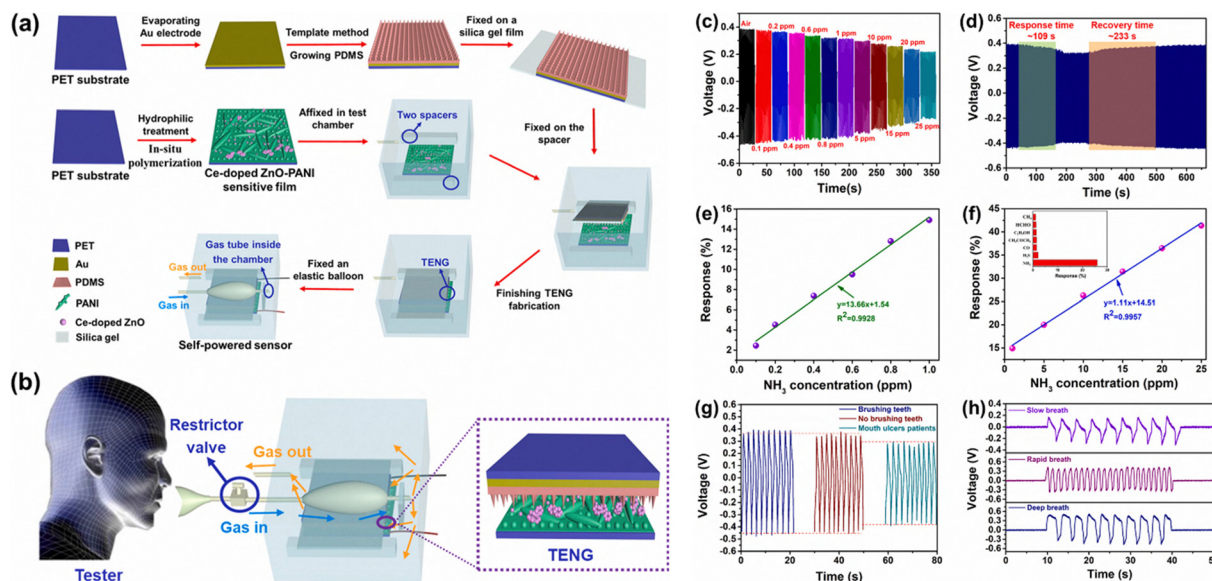
Fig. 6 (a) Schematic of the preparation process of the respiration-driven self-powered sensing system. (b) Schematic illustration of a human respiration-driven system. (c) Output voltages were detected at different NH_3 concentrations from 0.1 to 25 ppm at a fixed respiratory flow of 5 L min^{-1}. (d) Dynamic response of the Ce-doped ZnO-PANI sensitive film-based sensor for 1 ppm NH_3. (e) Response–NH_3 concentration fitting curve of the self-powered respiratory NH_3 sensor at 0.1–1 ppm NH_3. (f) Response–NH_3 concentration fitting curve of the NH_3 sensor at 1–25 ppm NH_3. Inset: Selectivity of the NH_3 sensor when exposed to 10 ppm NH_3 and other interference gases. (g) Comparison of output voltages in different oral environments at a fixed respiratory flow of 5 L min^{-1}. (h) Real-time respiratory signals of the TENG under three different human breathing behaviors without restricting the respiratory flow. (Reprinted with permission,[46] Copyright 2019, Elsevier.)

stable hydrogel sensors capable of reliable NH_3 detection in humid environments (Fig. 7). At 80% RH, the optimized sensors demonstrated outstanding selectivity for NH_3 over other interfering gases, a high response ratio ($Z_a/Z_g = 6.20$) at 20 ppm NH_3, and an exceptionally low detection limit of 50 ppb at RT. The enhanced chemical stability of the sensors was attributed to the balanced water content of the hydrogel matrix and the suitable acid dissociation constants of the embedded organic acids. The NH_3 sensing mechanism, activated by moisture, was comprehensively analysed through CIS, QCM studies, Fourier-transform infrared (FT-IR) spectroscopy, and X-ray photoelectron spectroscopy (XPS). Furthermore, the practical potential of these cross-linked hydrogel sensors for breath analysis was assessed through simulated exhaled breath experiments.

High ammonia (NH_3) levels in exhaled breath are important biomarkers for diagnosing end-stage renal disease. However, the complex composition and high moisture content of exhaled breath pose major challenges for accurate NH_3 sensing. To address this, Liu et al.[48] developed a humidity-activated sensing strategy that enables NH_3 detection at RT through a selective carboxylate formation reaction under high-humidity conditions. They fabricated an eco-friendly and non-toxic hydrogel sensor using poly-L-aspartic acid (PAA) and L-glutamic acid (GA) as functional materials. The sensor demonstrated a high response of 9.2 toward 50 ppm NH_3 at 80% RH, achieving outstanding sensitivity and selectivity. Detailed investigations revealed that the sensing mechanism involves a combination of acid–base adsorption, ionic conduction, and carboxylate formation driven by NH_3 interactions. This PAA/GA-based hydrogel sensor presents a new, highly selective

approach for ammonia detection in humid environments, offering great potential for non-invasive medical diagnostics through exhaled breath analysis.

Developing fabric-based nanogenerators with high output and continuous power delivery remains a major hurdle for advancing self-powered wearable electronics. To tackle this, Veeralingam et al.[49] introduced a cost-effective, lead-free TENG featuring hydrothermally synthesized titanium (Ti)-functionalized molybdenum disulfide (MoS_2) distributed within a polypropylene (PP) fabric, layered with a nylon sheet to create a highly sensitive system for respiration monitoring and NH_3 gas detection (Fig. 8). The Cu/Ti@MoS_2/PP: Nylon/Ag device structure was integrated into a respiratory mask, delivering an open-circuit voltage (V_{oc}) of 29.3 V and a short-circuit current density (J_{SC}) of 42.7 μA cm^{-2} during breathing cycles, successfully distinguishing various breath patterns. Additionally, by coupling the TENG with a Ti@MoS_2/PP-based ammonia sensor, a fully self-powered gas sensing system was developed. This sensor demonstrated excellent performance across a wide concentration ranging from 200 to 2600 ppb at RT, offering high sensitivity, selectivity, and fast response time. The work showcases the dual functionality of Ti@MoS_2 nanoparticles, establishing a promising platform for wearable respiratory tracking and self-powered health diagnostics, advancing next-generation smart healthcare technologies.

Furthermore, Sardana et al.[50] used first-principles density functional theory (DFT) simulations to systematically investigate an edge-site-enriched MXene/MoS_2 nanosheet heterostructure and found it effective as both the sensing material and the active layer in a hybrid triboelectric–piezoelectric nanogenerator
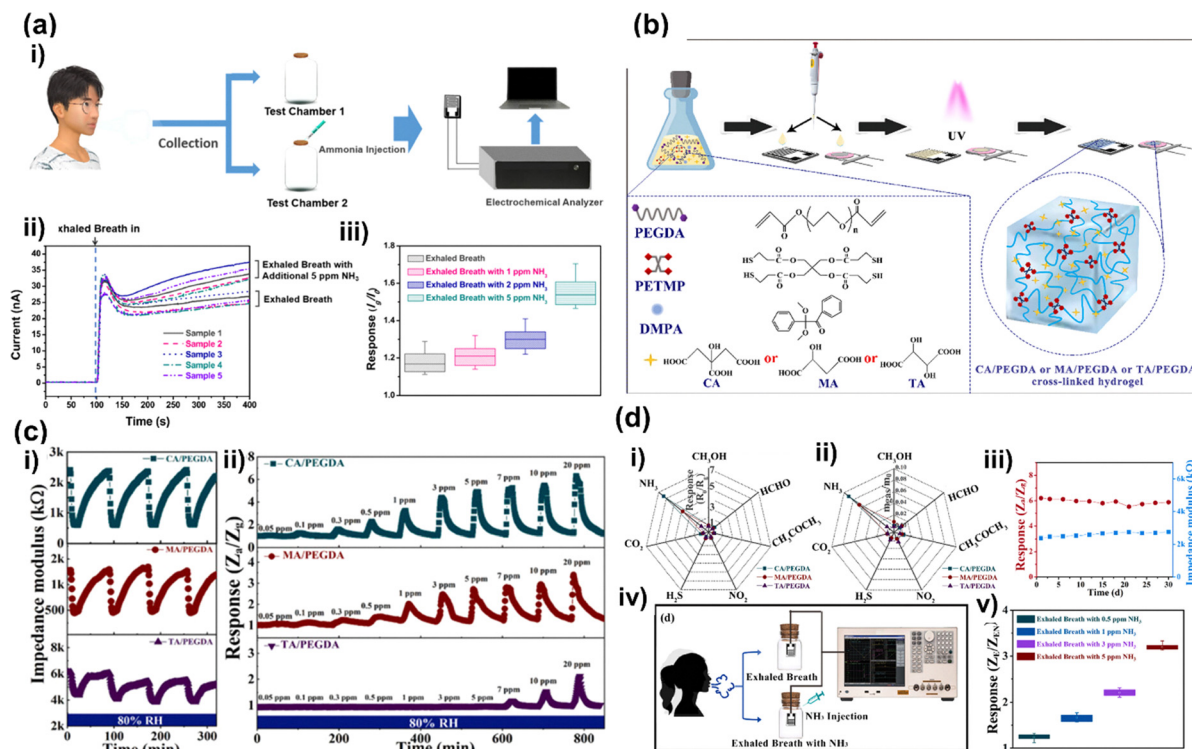
Fig. 7 (a) Ammonia-sensing process of the PVP sensor for real breath analysis. (i) Experimental procedures for breath analysis. (ii) Current−time curves for the PVP sensor in the normal exhaled breath of five testers and their exhaled breath with 5 ppm additional ammonia. (iii) Response characteristic of the PVP sensor to normal exhaled breath and exhaled breath with additional ammonia (n = 5). (Reprinted with permission,[7] Copyright 2020, ACS.) (b) Schematic of the preparation of the cross-linked hydrogel gas sensor. (c) (i) The response and recovery curve of CA/PEGDA, MA/PEGDA, and TA/PEGDA sensors to 20 ppm NH_3 at 80% RH; (ii) dynamic NH_3-sensing performance of CA/PEGDA, MA/PEGDA, and TA/PEGDA sensors in the concentration range of 0.05−20 ppm at 80% RH. (d) (i) The response and (ii) the adsorption ability of CA/PEGDA, MA/PEGDA, and TA/PEGDA to NH_3, CO_2, CH_3OH, H_2S, CH_3COCH_3, HCHO, and NO_2; (iii) long-term stability of the CA/PEGDA sensor over 30 days. The response (red) of the CA/PEGDA sensor to 20 ppm NH_3 at 80% RH and impedance modulus (blue) of the CA/PEGDA sensor at 80% RH; (iv) experimental procedures for the simulated breath analysis; (v) the response of the CA/PEGDA sensor in the normal exhaled breath of ten testers and their exhaled breath with different concentrations of NH_3. (Reprinted with permission,[47] Copyright 2021, Elsevier.)

(H-TPNG) (Fig. 9). This study proposes a NH_3 monitoring system designed for real-time breath sampling and environmental gas sensing. This novel integration enables the simultaneous realization of gas sensing and energy harvesting, facilitating a self-powered NH_3 monitoring system. The sensor exhibits high selectivity, reversibility, and sensitivity (47%@10 ppm) toward NH_3, attributed to the increased adsorption sites and enhanced charge transfer at the edge sites, as confirmed by DFT studies. In parallel, the mechanical tapping and bending motions of the H-TPNG effectively generate triboelectric and piezoelectric power densities of 1604.44 and 15.62 mW cm^{-2}, respectively, ensuring a sustainable energy supply for sensor operation. Additionally, the nanofibrous morphology introduced *via* electrospinning enhances the flexibility and conformability of the device, allowing seamless integration with large-area body-worn systems. Finally, a fully self-powered NH_3 monitoring system is assembled, demonstrating autonomous operation for both breath analysis and environmental gas detection. This study lays the foundation for the next generation of wearable gas sensors, paving the way for advanced self-sustained healthcare monitoring solutions.

In another study, Wang *et al.*[51] proposed a highly ultrasensitive self-powered NH_3 sensing system based on a vertical contact-separation mode TENG for RT detection in both ambient environments and human exhaled gases (Fig. 10). By leveraging the unique output characteristics of the TENG, which are finely tuned by the load resistance of the NH_3 sensor, the output voltage of the fabricated sensor exhibits a proportional relationship with NH_3 concentration, forming the core working principle of this self-powered gas sensing system. The triboelectric ammonia sensor (TEAS), developed using a PANI-MWCNTs composite thin film, demonstrates an exceptional NH_3 sensing response of 10% at an ultra-low concentration of 0.01 ppm, with a remarkable 255% response at 100 ppm NH_3. Additionally, the TEAS features fast response/recovery times (89−120 s/103−127 s for 0.6−100 ppm NH_3), excellent long-term stability, high selectivity, and robust anti-bending properties, ensuring durability in wearable applications. Furthermore, a preliminary trial for detecting NH_3 in human exhaled breath has been conducted, further extending the practical applications of the TEAS in non-invasive diagnostics. The results highlight the sensor's potential for ultrasensitive NH_3 monitoring, significantly expanding the applicability of TENG-based systems for human kidney health assessment by enabling a direct comparison of exhaled NH_3 concentration between
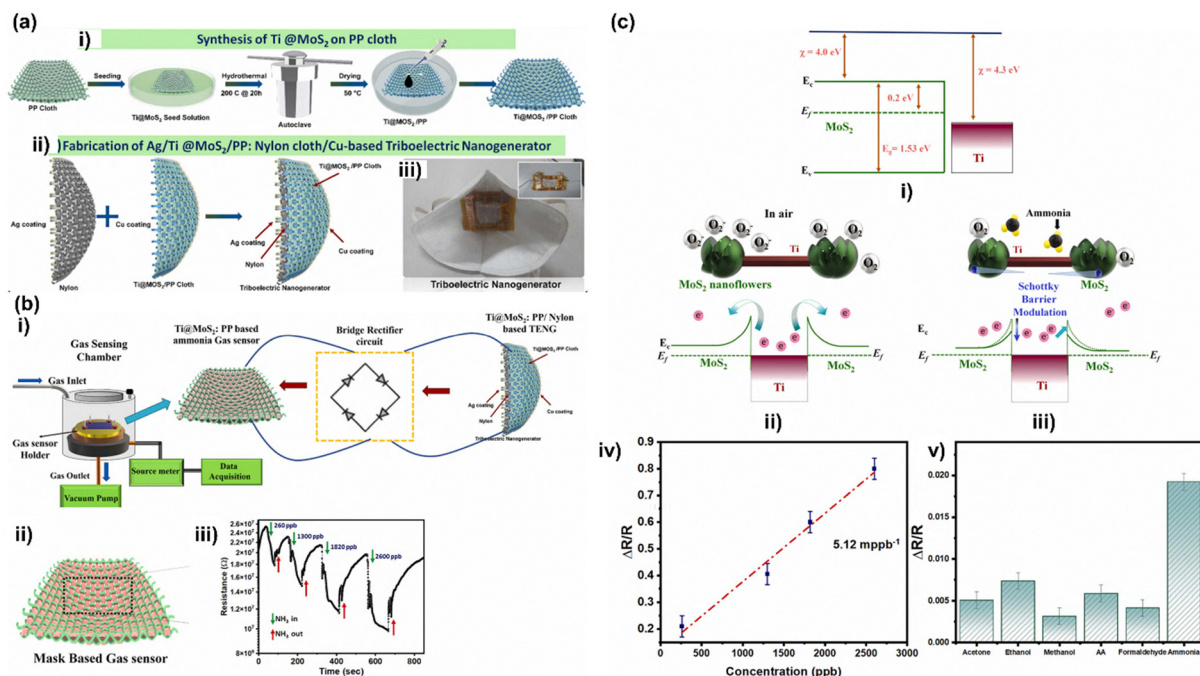
Fig. 8 (a) (i) Synthesis of Ti@MoS$_2$ on PP Cloth, (ii) steps for the fabrication of the Ag/Ti@MoS$_2$:PP/Nylon/Cu triboelectric nanogenerator, and (iii) real-time representation of the triboelectric mask nanogenerator. (b) (i) Schematic of the gas sensing chamber and the integrated self-powered ammonia gas sensing setup, (ii) schematic displaying the structure of the mask-based gas sensor, and (iii) the dynamic gas sensing response towards an increase in the concentration of ammonia. (c) (i) Band diagram of the Ti@MoS$_2$ structure; charge transport mechanism and band diagram of the Ti@MoS$_2$ gas sensor in an (ii) air atmosphere and (iii) ammonia atmosphere; (iv) calibration plot of the gas sensor displaying a sensitivity of 0.512 ppb^{-1}; and (v) selectivity studies towards co-existing species. (Reprinted with permission,[49] Copyright 2023, Elsevier.)

healthy individuals and potential patients. This study provides a pioneering approach to integrating self-powered sensing with real-time health monitoring, paving the way for next-generation biomedical diagnostic technologies.

3.3. Nitrogen dioxide (NO$_2$) gas sensors

Nitrogen dioxide (NO$_2$) represents a hazardous air pollutant predominantly generated from the burning of fossil fuels, resulting in respiratory ailments and detrimental environmental effects. The development of wearable, self-powered gas sensors is crucial for real-time NO$_2$ detection and breath analysis. Su *et al.* recently introduced an alveolus-inspired membrane sensor (AIMS), a triboelectric gas sensor employing a mechanically responsive structure and electrostatic induction for highly sensitive and selective NO$_2$ detection.[52] The AIMS device is designed with a vertically laminated structure, consisting of four key components: a latex film, a WO$_3$ sensing layer, a copper electrode, and a plastic air conduit (shown in Fig. 11a). The latex film, chosen for its excellent stretchability and electron affinity, functions as the triboelectric contact layer. The WO$_3$ sensing film, which serves as the active material for NO$_2$ detection, undergoes chemical modification using NaOH treatment, enhancing its adsorption capability. Studies have shown that a 0.02 g NaOH-treated WO$_3$ layer exhibits the highest sensitivity and response linearity compared to untreated or heavily treated films. The copper electrode and the plastic conduit facilitate charge collection and gas flow,

respectively. This structural design effectively mimics the human alveolus, enabling efficient gas exchange and charge separation.

A photograph of the as-fabricated AIMS is presented in Fig. 11a, illustrating the structural deformation of the latex membrane during gas inflation and deflation. As gas is introduced, the latex membrane expands, forming a tent-like structure, whereas upon deflation, it contracts back to its original state. This cyclic movement allows the latex film to undergo continuous contact and separation with the underlying WO$_3$ sensing layer, driving electron transfer between the copper electrode and the ground. This dynamic triboelectric-electrostatic process forms the basis of the AIMS working mechanism (illustrated in Fig. 11b(i–iv)). The difference in electron affinities between the latex film and the WO$_3$ layer induces charge transfer, resulting in positive charging of the WO$_3$ surface and negative charging of the latex film. As NO$_2$ gas enters the sensor, its strong electron affinity (2.27 eV) enables it to extract free electrons from the WO$_3$ film, altering the local charge distribution and reducing the internal depolarization field. This enhances the triboelectric output signal, and as the latex membrane expands and contracts, the induced electric potential varies, generating an alternating current that correlates with NO$_2$ concentration. The self-powered AIMS is ideal for portable and wearable applications because it requires no external power source.

The AIMS demonstrates exceptional NO$_2$ sensing capabilities, as highlighted in Fig. 11c. The response to NO$_2$ gas at
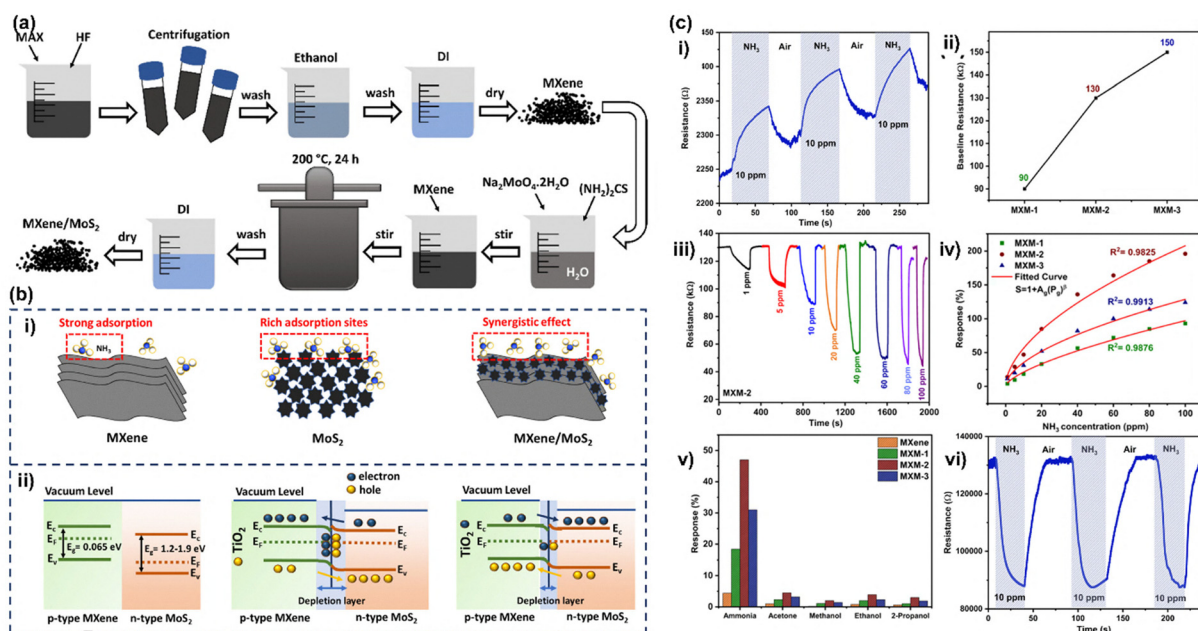
Fig. 9 (a) Schematic illustration of the two-step synthesis route for MXM nanocomposites. (b) (i) Schematic illustration of the proposed gas sensing mechanism and (ii) energy band diagrams related to interface modulation of MXene and MoS_2. (c) (i) Sensing curves (three continuous response–recovery cycles) of the pristine MXene-based sensor to 10 ppm NH_3, (ii) baseline resistance of the prepared nanocomposite (MXM-1, MXM-2, and MXM-3)-based sensor, (iii) sensing curves of the MXM-2 nanocomposite-based sensor to different concentrations of NH_3, (iv) fitting equations of the prepared sensors between the NH_3 concentration and response, (v) histogram depicting the comparison of responses of all prepared sensors to different gases, and (vi) sensing curves (three continuous response–recovery cycles) of the MXM-2 based sensor to 10 ppm NH_3. (Reprinted with permission,[50] Copyright 2022, ACS.)
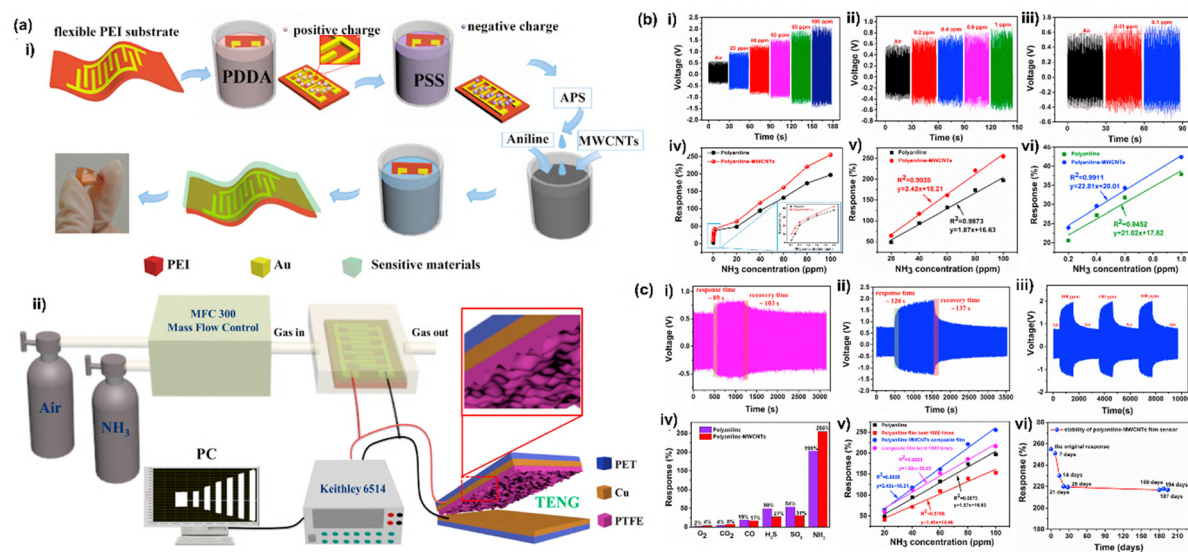

Fig. 10 (a) (i) The preparation schematic of the flexible NH_3 gas sensor based on a PANI-MWCNTs composite thin film; (ii) the sketch of the dynamic self-powered test system. (b) The output voltage for the PANI-MWCNTs composite film sensor when exposed to (i) 20–100 ppm NH_3, (ii) 0.2–1 ppm NH_3, and (iii) 0.01–0.1 ppm NH_3; (iv) the response curves of the two prepared sensors at 0.01–100 ppm NH_3. Inset: The response curves of the two prepared sensors at 0.01–1 ppm NH_3; (v) the response–concentration fitting curves of the two prepared sensors at 20–100 ppm NH_3; and (vi) the response–concentration fitting curves of the two prepared sensors at 0.2–1 ppm NH_3. (c) Dynamic response of the PANI-MWCNTs composite film sensor for (i) 0.6 ppm NH_3 and (ii) 100 ppm NH_3; (iii) repeatability of the PANI-MWCNTs composite film sensor upon alternate exposure to dry air and 100 ppm NH_3 for three cycles; (iv) the selectivity of PANI-MWCNTs and PANI film sensors when exposed to 100 ppm NH_3 and other gases; (v) the anti-bending ability of PANI film and PANI-MWCNTs composite film sensors after bending 1000 times; and (vi) the long term stability of the PANI-MWCNTs composite film sensor within the test time of 194 days. (Reprinted with permission,[51] Copyright 2018, Elsevier.)
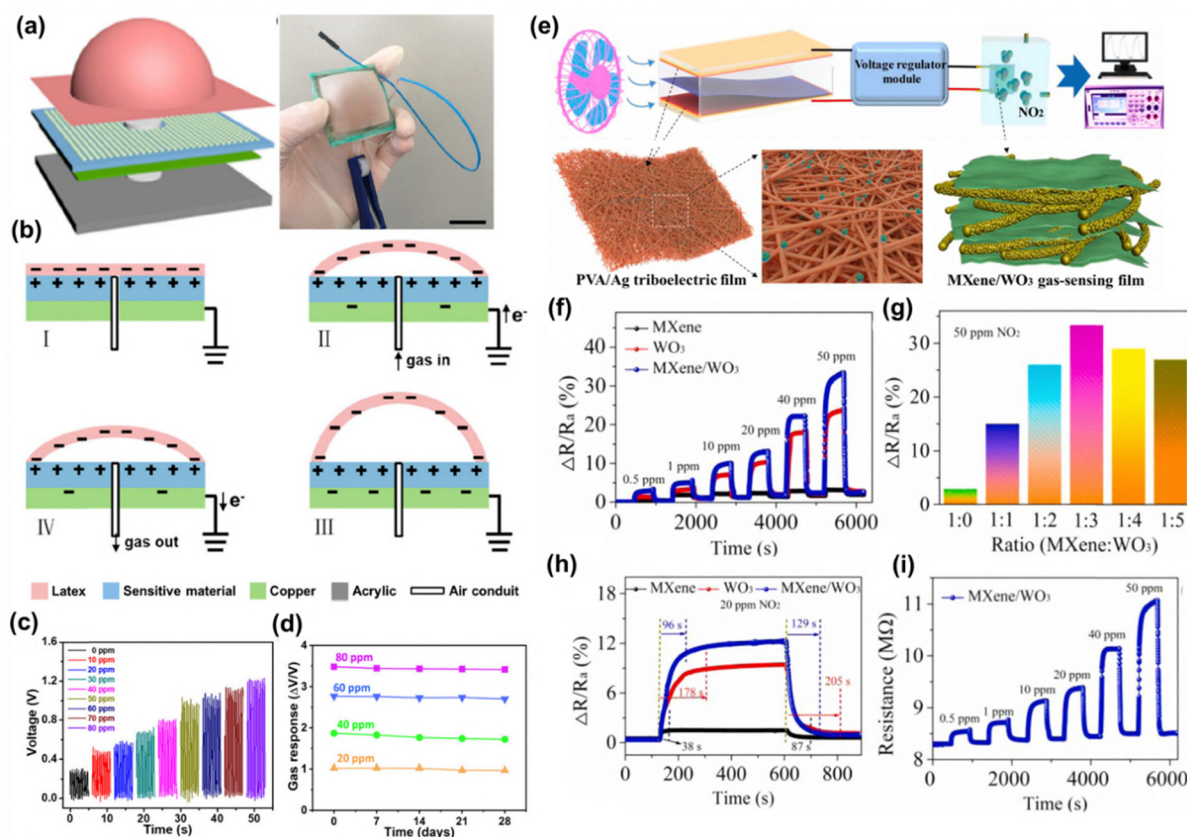
Fig. 11 (a) Schematic of the triboelectric nanogenerator-based AIMS gas sensor and its structure. (b) Working mechanism for the electricity generation of the AIMS. (c) Dynamic response of the AIMS with 0.02 g NaOH-treated WO_3 under different NO_2 concentrations. (d) Stability performance of the AIMS gas sensor over 24 days. Reproduced with permission,[52] Copyright © 2020, American Chemical Society. (e) Schematic illustration of the self-powered NO_2 sensor driven by a TENG. (f) The dynamic response variation ($\Delta R/R_a$) of the MXene, WO_3, and MXene/WO_3 sensors for varying NO_2 concentrations. (g) Sensitivity of the MXene/WO_3 sensor at different material ratios. (h) Response–recovery characteristics of the MXene/WO_3 sensor. (i) The dynamic resistance of the MXene/WO_3 sensor for different concentrations of NO_2. Reproduced with permission,[53] Copyright © 2022 Elsevier.

80 ppm reaches 340.24%, showcasing its high sensitivity. Furthermore, the sensor maintains a strong linear relationship (R^2 = 0.992) across different NO_2 concentrations, indicating its quantitative reliability. A critical aspect of gas sensors is their long-term stability, as demonstrated in Fig. 11d. The AIMS exhibits less than 5% signal degradation over one month, proving its durability for prolonged environmental and biomedical applications. Additionally, the sensor's selectivity was tested against other gases, including CO, CO_2, H_2S, SO_2, and NH_3, where the NO_2 response was at least 20 times higher than the response to these interfering species. This superior selectivity ensures reliable NO_2 detection even in mixed-gas environments. Further theoretical analysis revealed that the sensing mechanism involves the interaction between NO_2 and oxygen adsorbates on the WO_3 surface. Oxygen molecules (O_2) initially adsorb onto the WO_2 surface, capturing free electrons and forming $O_2(ads)^-$ species. When NO_2 interacts with these adsorbed oxygen ions, it extracts additional electrons, leading to a further reduction in free electron concentration and an increase in output voltage. The response and recovery times of the sensor were measured to be 273 and 330 s, respectively, showing a rapid adsorption and desorption when exposed to

NO_2 gas. The triboelectric charge transfer and the chemical adsorption effects synergistically contribute to the enhanced sensing performance of the AIMS, making it a highly efficient and self-sustained NO_2 detection system.

In another study, Wang *et al.* developed a self-powered NO_2 gas sensing system based on a wind-driven TENG and an MXene/WO_3 hybrid sensor.[53] Their work aims to develop a sustainable and highly sensitive platform for real-time environmental monitoring by integrating a polyvinyl alcohol/silver (PVA/Ag) nanofiber-based TENG with a $Ti_3C_2T_x$ MXene/WO_3 gas sensor. The system converts mechanical wind energy into electrical energy to power the NO_2 sensor, eliminating the need for external power sources. The MXene/WO_3 composite is chosen for its high conductivity, large surface area, and enhanced gas adsorption, improving the sensor response and recovery performance. The significance of this study lies in the development of an energy-harvesting gas sensor that can function efficiently under varying environmental conditions, offering a low-cost, maintenance-free, and sustainable approach for detecting harmful gases.

The schematic illustration of the system, as depicted in Fig. 11(e), highlights the working principle and structural

design of the wind-driven triboelectric nanogenerator and the NO_2 gas sensor. The PVA/Ag-based triboelectric film generates electrical output upon exposure to airflow, which is then regulated through a voltage regulation module to power the NO_2 sensor. The sensing material, MXene/WO_3 hybrid film, enhances the system selectivity and sensitivity towards NO_2 molecules, offering a real-time detection capability. The magnified views of the nanofibers confirm the uniform dispersion of Ag nanoparticles within the polymer matrix, improving the triboelectric charge transfer efficiency. Fig. 11(f) shows the dynamic response variation ($\Delta R/R_a$) of the MXene/WO_3 sensor for different NO_2 concentrations ranging from 0.5 to 50 ppm. The MXene/WO_3 sensor exhibits a higher response compared to pure MXene and WO_3-based sensors, confirming that the hybrid structure significantly improves gas-sensing efficiency. The sensor response increases with higher NO_2 concentrations, demonstrating its ability to detect varying gas levels accurately. Fig. 11(g) highlights the impact of different MXene-to-WO_3 mass ratios on the sensor's response at 50 ppm NO_2. The 1:3 MXene/WO_3 composition yields the highest response, indicating that this ratio optimally balances the conductivity of MXene and the gas adsorption capabilities of WO_3. This finding confirms that modifying the material composition is crucial for enhancing the sensor's performance. Fig. 11(h) presents the response and recovery time comparison for MXene, WO_3, and MXene/WO_3 sensors at 20 ppm NO_2. The MXene/WO_3 sensor exhibits faster response and recovery times (96/129 s) compared to WO_3 (178/205 s) sensor, confirming that the hybrid structure facilitates quicker electron transfer and gas adsorption/desorption cycles. This faster reaction time is essential for real-time NO_2 monitoring under dynamic environmental conditions. Fig. 11(i) displays the resistance variation of the MXene/WO_3 sensor as a function of NO_2 concentration over time. The resistance increases stepwise with increasing NO_2 levels, ensuring a stable and repeatable sensing performance. This linear response trend suggests that the sensor can be effectively calibrated for precise NO_2 quantification.

The novelty of this work lies in the innovative integration of a TENG with an MXene/WO_3 nanohybrid gas sensor, creating a self-powered system that significantly advances beyond traditional sensors requiring external power sources. This self-powered sensor demonstrates an exceptional response to NO_2 gas, with a response rate 15 times greater than that of conventional resistive sensors, showcasing the effectiveness of the TENG-driven system. Additionally, the use of wind energy to power the TENG introduces a sustainable and maintenance-free energy solution, capable of maintaining a constant voltage output across a wide range of wind speeds and humidity levels, which is a unique feature not commonly found in similar technologies. Furthermore, the development of a multifunctional detection system capable of detecting both wind direction and NO_2 gas is a novel contribution, offering a comprehensive solution for environmental monitoring by tracing the source of harmful gases. This sustainable detection platform, which does not require frequent maintenance, enhances its practicality and application potential in real-world environmental monitoring scenarios.

Further, Su *et al.* introduced a UV-activated self-powered NO_2 detection system, where a TENG-driven chemoresistive gas sensor based on ZnO–reduced graphene oxide (ZnO–RGO) hybrid films detects NO_2 with high sensitivity at RT.[54] The novelty of their work lies in the integration of UV activation, which enhances photo-induced charge separation, leading to superior NO_2 adsorption and an amplified sensing response. The ZnO–RGO composite-based sensor exhibited a 49 times higher response to NO_2 compared to other gases, confirming its exceptional selectivity and reliability. Furthermore, they introduced a real-time NO_2 gas alert system, which automatically processes sensor signals to notify users of hazardous NO_2 levels, making it highly suitable for environmental air quality monitoring and industrial safety applications.

Recently, Das *et al.* developed a cobalt nanocluster-decorated nitrogen-doped graphene (Co–N–Gr) triboelectric sensor for real-time NO_x detection and respiratory monitoring in asthma patients.[55] The authors developed a dual-mode sensing capability, where the sensor not only detects NO_x content but also monitors human respiratory strength, distinguishing between different breathing patterns such as deep mouth breath, deep nasal breath, and normal nasal breath. This sensor is highly significant for biomedical applications, particularly for early-stage asthma diagnosis. By leveraging cobalt nanocluster doping, the sensor achieves ultrafast response and recovery times of 1.16 and 1.39 s, respectively, which align with normal human breathing frequencies. Moreover, the sensor operates under zero-bias conditions, meaning it can function without any external power supply, making it a cost-effective and wearable diagnostic tool. These TENG-driven gas sensors not only enhance detection performance and durability but also pave the way for next-generation self-sustained sensor networks, bridging the gap between wearable health monitoring and large-scale environmental surveillance.

3.4. Formaldehyde (HCHO) gas sensor

Formaldehyde (HCHO) detection is crucial due to its toxic and carcinogenic nature, which pose serious health risks such as respiratory issues, neurological effects, and cancer. As a major indoor air pollutant, formaldehyde is commonly emitted from sources such as furniture, adhesives, and household products, contributing to sick building syndrome (SBS). Continuous monitoring of formaldehyde levels is particularly critical in industries such as wood processing, healthcare, and chemical manufacturing; therefore, the detection of formaldehyde has become vital in many sectors.[56]

Wang *et al.* have developed a self-powered multifunctional formaldehyde sensor using a respiration-driven TENG based on $Ti_3C_2T_x$ MXene/amino-functionalized multi-walled carbon nanotubes (MXene/NH_2-MWCNTs).[57] The system functions as both a power source and a formaldehyde sensor, making it an eco-friendly, energy-efficient, and portable device for real-time gas detection. The MXene/NH_2-MWCNTs composite serves as both a triboelectric friction layer and an electrode, providing an active surface for formaldehyde adsorption and charge transfer. As shown in Fig. 12(a), the system is powered by human respiration, where the breathing motion drives the TENG to
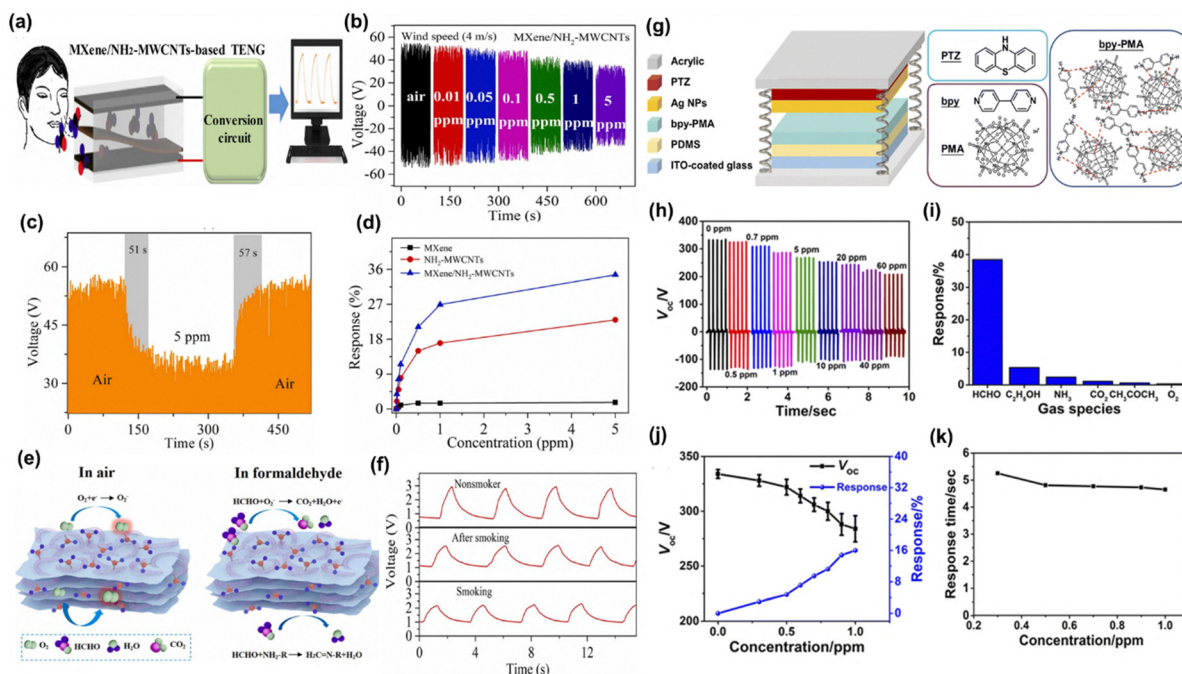
Fig. 12 (a) Application diagram of the MXene/NH$_2$-MWCNTs-based TENG. (b) The output voltage under different formaldehyde concentrations. (c) The response and recovery time of the self-powered sensor. (d) The response of the three prepared self-powered sensors. (e) The gas-sensing mechanism of the MXene/NH$_2$-MWCNTs composite. (f) The charge voltage of the capacitor when the TENG was driven by the respiration of the tester in different states (nonsmoker, smoking, and after smoking). Reproduced with permission,[57] Copyright © 2022 Elsevier. (g) Schematic illustration of the TENG architecture and chemical structure of the materials investigated in this work. (h) FA concentration-dependent Voc output of the sensors. (i) Selectivity of the sensors for different target gases. (j) FA concentration-dependent Voc output and response values of the sensors. (k) FA concentration-dependent response time of the sensors. Reproduced with permission,[58] Copyright © 2022 Royal Society of Chemistry.

generate electrical output, which is then processed through a conversion circuit for gas sensing applications. The TENG can generate a peak-to-peak open-circuit voltage of 136 V and an output power of 27 μW, ensuring a stable self-sustained energy source.

The gas sensing performance of the device is highly effective, as shown in Fig. 12(b), where the voltage output varies with increasing formaldehyde concentrations from 0.01 to 5 ppm. The sensor demonstrates a high sensitivity of 35% at 5 ppm, with a low detection limit of 10 ppb and a rapid response/recovery time of 51 s/57 s, as illustrated in Fig. 12(c). This makes the sensor highly suitable for detecting formaldehyde in exhaled breath, particularly in smokers. The response curve in Fig. 12(d) compares different material compositions (pure MXene, NH$_2$-MWCNTs, and MXene/NH$_2$-MWCNTs), confirming that the MXene/NH$_2$-MWCNTs composite has the highest response, demonstrating its enhanced gas adsorption and charge transfer efficiency.

The sensing mechanism is further explained in Fig. 12(e), showing the interaction between formaldehyde molecules and the MXene/NH$_2$-MWCNTs composite. In an air environment, oxygen molecules (O$_2$) adsorb onto the sensing material, forming oxygen species (O$_2^-$), which capture free electrons and create a depletion layer. When formaldehyde is introduced, it acts as a reducing agent, reacting with the adsorbed oxygen species and releasing electrons back into the conduction

band, reducing resistance and increasing voltage output. The presence of NH$_2$ groups enhances this reaction, further improving formaldehyde detection.

Beyond gas sensing, the respiration-driven TENG is also employed for human respiratory monitoring, with significant applications in disease diagnosis. As depicted in Fig. 12(f), the system can distinguish different breathing patterns among nonsmokers, post-smoking individuals, and active smokers, showing variations in voltage output. The voltage fluctuation in smokers is more irregular, which can be attributed to lung function impairment due to formaldehyde and other toxic compounds in cigarette smoke. The system can also detect various respiratory patterns, such as normal, rapid, slow, Cheyne-Stokes, and Biot breathing, all of which are associated with specific medical conditions like cardiovascular diseases, brainstem lesions, and sleep disorders. Using a support vector machine (SVM) model, the sensor achieved 100% accuracy in classifying different respiratory types, highlighting its capability as a wearable, non-invasive diagnostic tool. The integration of MXene/NH$_2$-MWCNTs with triboelectric nanogenerators enables ultrasensitive formaldehyde detection, real-time monitoring of human breath, and energy autonomy, making it a promising solution for air quality monitoring, disease diagnosis, and biomarker detection in clinical settings.

Recently, Chang *et al.* have developed a room-temperature, high-performance self-powered formaldehyde sensor utilizing a

monolithic TENG, which enables both energy harvesting and gas sensing without external power sources.[58] Their work introduced a novel surface-engineered sensing material, combining 4,4′-bipyridine-functionalized phosphomolybdic acid (bpy-PMA) with phenothiazine (PTZ)-modified silver nanoparticles (Ag NPs), resulting in unprecedented formaldehyde sensitivity and selectivity at RT.

The sensor structure and material composition are detailed in Fig. 12(g), where a bpy-PMA/PDMS triboelectric layer and a PTZ/Ag NP electrode facilitate efficient triboelectric charge generation and formaldehyde adsorption. This design achieved an open-circuit voltage of 332 V, a short-circuit current of 32.8 µA, and a transferred charge of 21.9 nC, ensuring long-term stability over 200 000 cycles. The integration of bpy-PMA enhances moisture resistance, making the sensor highly stable under varying environmental conditions.

The sensor's real-time response to formaldehyde concentrations is illustrated in Fig. 12(h), where voltage fluctuations correlate directly with formaldehyde levels from 0.5 to 60 ppm, proving its ultra-fast response time of approximately 5 s, which is significantly faster than conventional sensors. The selectivity study in Fig. 12(i) further confirms that the sensor exhibits a 130-fold higher response to formaldehyde compared to interfering gases such as ethanol, ammonia, CO, and acetone, demonstrating its superior gas discrimination ability. This is attributed to the strong oxidizing nature of bpy-PMA, which enhances electron transfer between formaldehyde molecules and the sensing surface. The concentration-dependent sensor response is detailed in Fig. 12(j), showing a linear increase in formaldehyde response with concentration, confirming its high sensitivity even at sub-ppm levels. The sensor response time, shown in Fig. 12(k), remains stable across different concentrations, indicating a robust and reproducible sensing performance. The fast response and recovery dynamics are due to the highly reactive surface sites of bpy-PMA, promoting rapid formaldehyde adsorption and desorption.

A breakthrough aspect of this study is the real-time, self-powered formaldehyde detection in a wearable mask, demonstrating the feasibility of non-invasive monitoring of formaldehyde exposure through exhaled breath. This innovation is particularly valuable for occupational safety, lung disease diagnosis, and air quality monitoring. The wearable facemask prototype processes real-time voltage signals, correlating with airflow to enable continuous, hands-free formaldehyde monitoring. This work represents a significant advancement in TENG-driven gas sensors, offering sustainable, real-time, and ultra-fast formaldehyde detection with potential applications in air quality control, industrial safety, and biomedical health monitoring.

3.5. Hydrogen sulfide (H$_2$S) gas sensor

Hydrogen sulfide (H$_2$S) is a highly toxic, flammable, and corrosive gas commonly found in oil refineries, wastewater treatment plants, natural gas processing, and industrial manufacturing. Real-time H$_2$S gas sensing is crucial.[59]

Huang *et al.* have developed a self-powered, stretchable hydrogen sulfide (H$_2$S) sensor utilizing a Zn/Ag-based electrochemical mechanism combined with a hydrogel electrolyte.[60] This sensor offers real-time, ultra-sensitive, and selective H$_2$S detection at RT without requiring external power sources. The device operates through a spontaneous electrochemical potential change when exposed to H$_2$S, generating a detectable voltage shift correlating with gas concentration. Unlike conventional gas sensors, which often demand high operating temperatures and significant power consumption, this innovative sensor is low-energy-consuming, highly stable, and flexible, making it highly suitable for wearable devices, food safety monitoring, and industrial air quality assessments. The sensor demonstrated high selectivity against interfering gases, exceptional long-term stability, and reliable performance under varying humidity and temperature conditions. Furthermore, its effectiveness in detecting food spoilage was verified, as it accurately tracked H$_2$S emissions from decaying meat, providing a real-time assessment of food freshness.

The structure and working mechanism of the sensor are illustrated in Fig. 13(a); the sensor consists of Zn and Ag electrodes immersed in a hydrogel electrolyte, forming a galvanic cell that generates a stable open-circuit voltage (OCV). When H$_2$S interacts with the Ag electrode, a surface reaction alters the electrode's potential, causing a measurable voltage shift. This process allows real-time, energy-free detection of H$_2$S, making it ideal for portable and wearable environmental monitoring applications. The comparative study in Fig. 13(b) highlights the sensor's superior response using a Zn/Ag electrode pair, which outperforms alternative configurations such as Zn/Fe and Fe/Ag due to its strong electrochemical reactivity with H$_2$S.

The sensor's dynamic response to different H$_2$S concentrations, shown in Fig. 13(c), reveals a proportional voltage shift corresponding to gas concentration, confirming its repeatable and quantifiable detection ability. This figure also includes different glycerol-modified hydrogel variations, indicating that hydrogel modifications can enhance sensing response and durability. The long-term stability of the sensor, as presented in Fig. 13(d), demonstrated minimal degradation over 20 days, verifying its robust performance for extended monitoring applications. Additionally, the signal degradation analysis in Fig. 13(e) confirms that the Zn/Ag-based sensor maintains better long-term stability than Zn/Fe, indicating enhanced electrode resilience.

The effects of humidity on sensing performance are presented in Fig. 13(f and g), which shows that while higher humidity levels slightly reduce sensitivity, the sensor still maintains consistent detection accuracy. The temperature-dependent response is illustrated in Fig. 13(h and i), which indicates that the sensor remains highly stable across a wide range of environmental temperatures (−20 to 40 °C), making it suitable for applications in cold storage, industrial safety, and extreme environmental monitoring.

One of the most promising applications of this sensor is food spoilage monitoring, as demonstrated in Fig. 13(j), where the device successfully detects H$_2$S emissions from degrading pork, distinguishing between a blank control sample and an experimental group. The real-time tracking of voltage variations due to the decomposition of meat, shown in Fig. 13(k), confirms its ability to function as a non-invasive, reliable tool for
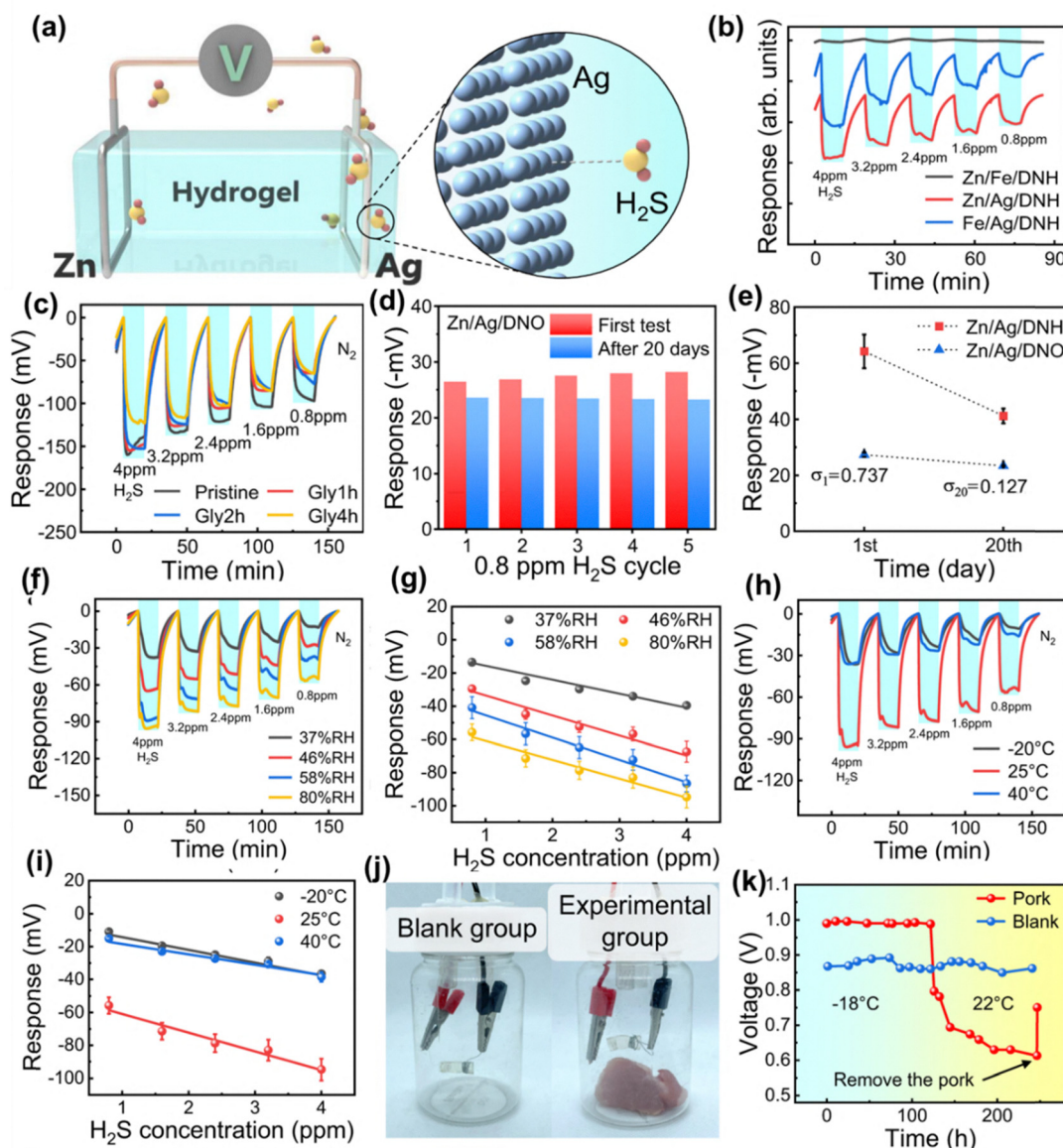
Fig. 13 (a) Schematic illustration of the self-powered H$_2$S sensor based on Zn/Ag electrodes and a hydrogel electrolyte. (b) Comparison of H$_2$S sensing responses for different electrode configurations (Zn/Ag, Zn/Fe, and Fe/Ag). (c) Dynamic response of the sensor to various H$_2$S concentrations (0.8−4 ppm) with different hydrogel modifications. (d) Long-term stability test showing sensor response over 20 days with repeated H$_2$S exposure cycles. (e) Signal degradation analysis of Zn/Ag and Zn/Fe electrodes over time under continuous H$_2$S exposure. (f) Humidity-dependent response of the sensor across different relative humidity (RH) levels. (g) Sensitivity comparison of the sensor under varying humidity conditions (37−80% RH). (h) Temperature-dependent H$_2$S sensing response at −20 °C, 25 °C, and 40 °C. (i) Effect of temperature variations on sensor response across different H$_2$S concentrations. (j) Application of the sensor in food spoilage detection, comparing a blank group with pork samples. (k) Real-time voltage response of the sensor during food spoilage monitoring, showing H$_2$S accumulation over time. Reproduced with permission,[60] Creative Commons Attribution 4.0 International License Copyright © 2023 Springer Nature.

assessing food freshness. The clear voltage drops over time correlate with increasing H$_2$S emissions, reinforcing its capability for food safety applications. In conclusion, the Zn/Ag electrochemical system allows for real-time H$_2$S detection, demonstrating broad applications in wearable healthcare devices, air quality monitoring, and food safety assessment. The integration of wireless monitoring technology further enhances its practical usability, making it a groundbreaking advancement in self-powered gas sensing technologies.

In another study, Liu *et al.* have developed a lever-inspired triboelectric respiration sensor (TRS) for simultaneous respiratory behavioral assessment and exhaled hydrogen sulfide (H$_2$S) detection.[61] This novel design enhances the flow sensitivity of triboelectric respiration sensors (TRSs) by leveraging an adjustable contact-separate mechanism between dielectrics, which is a more efficient and straightforward approach compared to conventional microstructure modifications or composite material engineering. The sensor incorporates an Fe^{2+}-doped

polypyrrole (FPPy) sensing film, which is self-assembled *in situ* on the electrode and interacts selectively with H_2S gas. The device functions by detecting impedance variations in the sensing layer, leading to measurable voltage changes that correlate with gas concentration. With an optimized power arm to resistance arm ratio of 1:2, the sensor demonstrates exceptional respiration monitoring capabilities, accurately measuring flow rates (0.5–8 L min^{-1}) and breathing frequencies (0.25–1 Hz). The H_2S sensing performance is also remarkable, exhibiting a high response of 25.21% at 10 ppm H_2S, excellent repeatability ($\pm0.46\%$), and a low detection limit of 1 ppm. Furthermore, the TRS successfully distinguishes exhaled H_2S from other respiratory gases, enabling non-invasive halitosis detection and vital sign monitoring.

The working principle of the sensor is based on a TENG mechanism, where a PTFE triboelectric negative film and a Cu–Ni electrode serve as the triboelectric layers. When the lever moves due to respiration flow, the induced charge separation generates an electric potential difference, which is further modulated by the impedance variations of the FPPy sensing film upon exposure to H_2S. The formation of conductive ferrous sulfide (FeS) due to Fe^{2+}–H_2S interactions enhances the conductivity of the sensing film, leading to a higher triboelectric output voltage. The sensor maintains excellent performance even in high-humidity environments (80% RH), demonstrating its suitability for real-world applications.

Additionally, the study explores the detailed sensing mechanism by analyzing *in situ* impedance variations, X-ray diffraction (XRD), and X-ray photoelectron spectroscopy (XPS) data. This analysis confirms that the interaction of H_2S with Fe^{2+} results in the reversible formation of FeS, which modifies the impedance of the sensing film and alters the TRS output voltage. The sensor also exhibits a selectivity factor of at least 2.6 times higher for H_2S compared to interfering gases such as NH_3, acetone, formaldehyde, and ethanol. In practical demonstrations, the TRS effectively detects exhaled H_2S from halitosis patients, with a 3.2% response increase upon exposure to 1 ppm H_2S in simulated halitosis breath. The lever-inspired design enhances mechanical flexibility and energy conversion efficiency, while the Fe^{2+}-doped polypyrrole sensing layer ensures highly sensitive and selective H_2S detection. The integration of biomechanical and biochemical sensing capabilities makes this TRS a promising tool for respiratory health monitoring, non-invasive disease diagnostics, and wearable biomedical applications.

3.6. Biomedical applications and disease diagnosis

Huang *et al.* presented a novel tubular surface-enhanced Raman scattering (SERS) sensor for non-invasive detection of gastric cancer using breath analysis.[62] Gastric cancer is one of the leading causes of cancer-related deaths, and current diagnostic techniques, such as gastroscopy and biopsy, are invasive and time-consuming. To address these limitations, the study explores an alternative approach that detects volatile organic compounds (VOCs) in exhaled breath, which serve as biomarkers for gastric cancer. The Ag@ZIF-67-based SERS sensor consists of silver nanoparticles (AgNPs) coated with a metal–organic framework

(MOF), ZIF-67, which enhances gas adsorption and Raman signal intensity. The sensor is further functionalized with 4-amino-thiophenol (4-ATP) to selectively capture aldehydes and ketones, enabling accurate and real-time detection of gastric cancer.

As shown in Fig. 14(a), the working principle of the tubular SERS sensor involves exhaled breath passing through a glass capillary filled with Ag@ZIF-67 nanoparticles, where VOCs interact with the sensor surface and produce distinct Raman signals upon laser excitation. The Raman spectrum of the captured VOCs is analyzed to determine whether the breath sample belongs to a gastric cancer patient or a healthy individual. The sensor acts both as a gas flow channel and a detection chamber, maximizing gas retention and ensuring efficient Raman signal enhancement. Fig. 14(b) compares the Raman spectra of gastric cancer patients and healthy individuals, highlighting the distinct spectral peaks corresponding to different VOC biomarkers. The green spectrum represents gastric cancer patients, while the blue spectrum corresponds to healthy individuals. The significant differences in Raman peak intensities indicate the presence of higher concentrations of specific aldehydes and ketones in gastric cancer patients, serving as diagnostic markers.

The sensor design is illustrated in Fig. 14(c), which shows the physical setup of the capillary sensor system. The capillary tube, packed with Ag@ZIF-67 nanoparticles, is positioned inside a transparent resin channel, allowing controlled airflow for efficient gas capture. This setup improves the adsorption efficiency of VOCs, ensuring high sensitivity and repeatability in Raman signal detection. To improve real-time diagnostic efficiency, the collected spectral data are converted into barcode representations, as shown in Fig. 14(d). The spectral data for gastric cancer (green) and healthy individuals (blue) are transformed into unique barcode signatures, enabling smartphone-based rapid diagnosis. This approach enhances the clinical applicability of the sensor, making it a potential tool for point-of-care testing. The detection mechanism of aldehydes and ketones is presented in Fig. 14(e). The chemical interaction between 4-ATP and benzaldehyde forms a Schiff base (C=N bond), which enhances the Raman signal at 1625 cm^{-1}. The bottom-left spectra in Fig. 14(e) demonstrate the Raman response of the sensor before and after VOC adsorption, showing a clear increase in peak intensities after exposure to gastric cancer biomarkers. The depth-resolved Raman mapping, also in Fig. 14(e), further confirms the localized adsorption of VOCs within the detection region. The "Before" and "After" images show stronger red-hotspots post-exposure, validating the high gas-capturing efficiency of the tubular sensor.

Huang *et al.* emphasized that the tubular SERS sensor offers several advantages over traditional diagnostic techniques. The integration of Ag@ZIF-67 nanoparticles and 4-ATP functionalization provides a highly selective and sensitive detection platform. Compared to conventional gas chromatography-mass spectrometry (GC-MS), which requires expensive and complex instrumentation, the SERS sensor achieves comparable accuracy within 20 min. Additionally, the barcode-based spectral
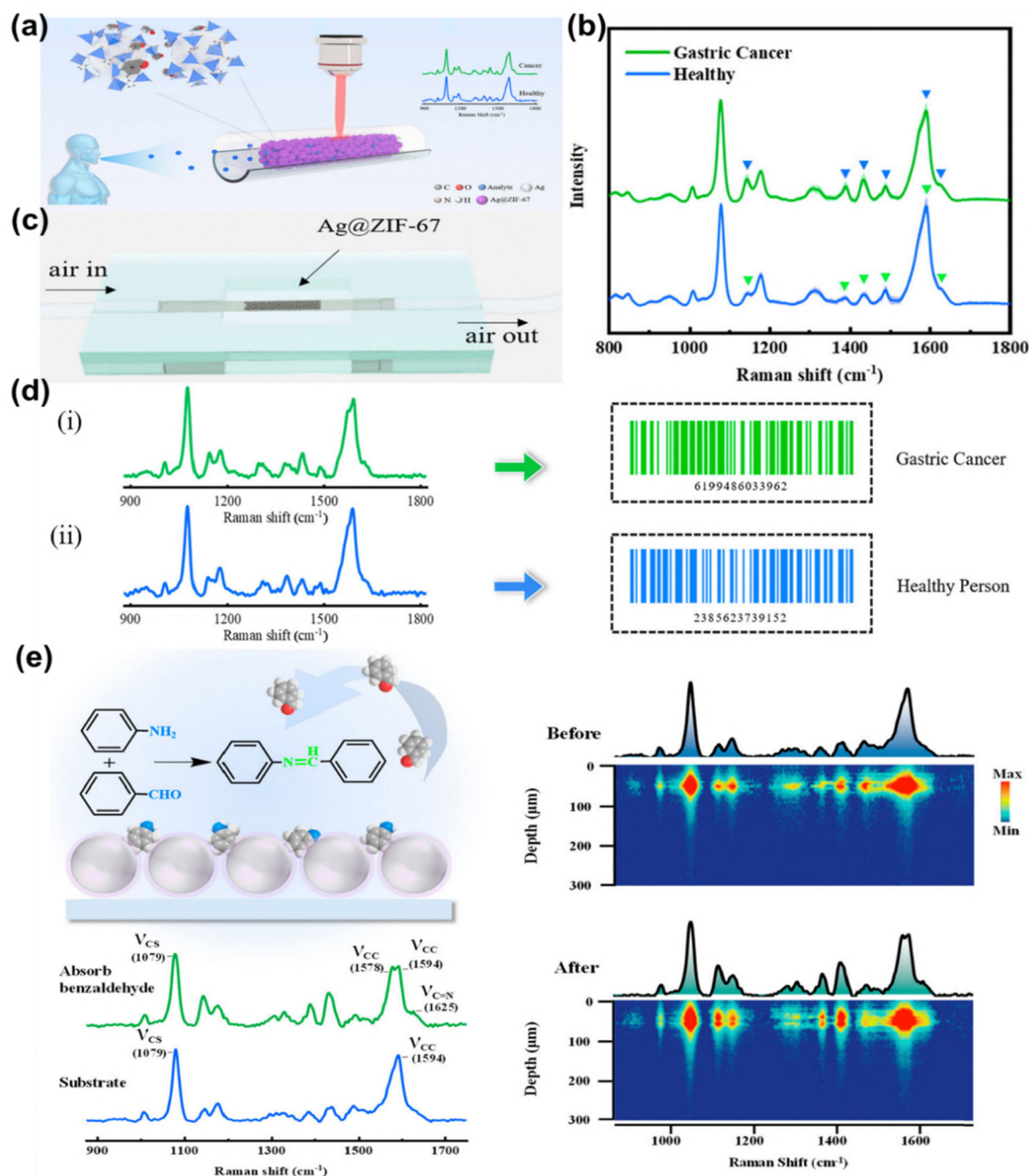
Fig. 14 (a) Schematic representation of the tubular SERS sensor for breath analysis, showing the detection mechanism of VOCs in exhaled air. (b) Comparison of Raman spectra from gastric cancer patients (green) and healthy individuals (blue), highlighting significant spectral differences in VOC biomarkers. (c) Structural setup of the tubular SERS sensor, showing the Ag@ZIF-67 nanoparticle-packed capillary integrated into the detection system. (d) Barcode conversion of Raman spectra for gastric cancer (green) and healthy individuals (blue), facilitating rapid and automated diagnosis. (e) Mechanism of aldehyde and ketone detection using 4-ATP-modified Ag@ZIF-67 nanoparticles and depth-resolved Raman intensity mapping before and after VOC adsorption. Reproduced with permission,[62] Copyright © 2022 American Chemical Society.

conversion makes the system adaptable for portable and real-time disease monitoring.

The study demonstrates the first successful application of a tubular SERS sensor for gastric cancer detection *via* breath analysis. The sensor's high accuracy (89.83%), rapid analysis, and noninvasive nature make it a promising tool for early

gastric cancer screening. Compared to traditional diagnostic methods, this approach offers a cost-effective, portable, and patient-friendly alternative with potential applications in real-time disease monitoring. The authors suggest that further clinical trials are necessary to validate the sensor's performance in large-scale populations and explore its applicability in

detecting other respiratory diseases. This SERS-based breath sensor could revolutionize non-invasive cancer screening, making early detection more accessible and efficient worldwide.

3.7. Oxygen (O$_2$) gas sensor

Lin *et al.* present a wearable exhaling-oxygen-sensing mask that integrates piezoelectric gas sensing with real-time wireless monitoring to assess lung function and oxygenation levels.[63] The mask consists of tetrapod ZnO (T-ZnO) nanostructures hybridized with polyvinylidene fluoride (PVDF) on a fabric substrate, enabling the detection of oxygen concentration in exhaled breath. The piezoelectric properties of T-ZnO/PVDF allow the conversion of breath energy into an electrical signal, eliminating the need for an external power source. The voltage output is proportional to oxygen concentration, enabling real-time monitoring of respiratory health. A Bluetooth module is integrated for wireless data transmission to external devices, making this self-powered, non-invasive, and portable sensor useful for continuous respiratory health assessment, early disease diagnosis, and remote healthcare applications.

Fig. 15(a) illustrates the self-powered sensing mask designed for real-time exhaled oxygen concentration monitoring. The schematic shows how exhaled breath passes through the gas-sensing layer, leading to oxygen adsorption, signal generation, and wireless data transmission. The mask detects oxygen concentration and generates voltage signals that are transmitted to a mobile device, which can provide warning alerts in cases of oxygen level drops, indicating potential respiratory issues. The fabrication process of the sensing unit is shown, where multiple layers, including silver paste electrodes, PVDF-doped T-ZnO, and polypropylene non-woven fabric, are assembled. The T-ZnO/PVDF composite is coated onto the fabric *via* a suspension process, ensuring strong adhesion and high sensing efficiency. The combination of piezoelectric and gas-sensing effects enhances the sensor's ability to detect variations in exhaled oxygen concentration.

Fig. 15(b) explains the working mechanism of the sensor, which relies on the piezoelectric-gas sensing coupling effect. The diagram illustrates how oxygen molecules interact with the T-ZnO nanostructures, altering the electron depletion layer. When the mask is worn and exhalation occurs, mechanical deformation of the sensor generates a piezoelectric voltage signal. In the absence of deformation, no significant voltage is generated, but during breathing, stretching and compression of the sensor lead to electron transfer and modulation of the voltage output. This mechanism allows for accurate detection of exhaled oxygen levels, making it suitable for real-time respiratory monitoring without the need for an external power source.

Fig. 15(c) presents experimental data demonstrating the sensor's response to varying oxygen concentrations. The upper graph shows that as the oxygen concentration increases from 10 to 50%, the voltage output also increases, confirming the sensor's high sensitivity and accuracy in detecting exhaled oxygen variations. The lower graph focuses on the oxygen range typical for human exhalation (10 to 20%), verifying the sensor's capability to detect small fluctuations in breath composition. The different colored bars represent multiple test cycles, showing the stability and repeatability of the sensor's performance. These results confirm that the mask can effectively monitor lung function and oxygenation levels in real-time. Fig. 15(d) illustrates the practical application of the self-powered wearable exhaling-oxygen-sensing mask for real-time monitoring and uploading lung oxygenation levels. The system is composed of an oxygen-sensing unit, a precision active peak detector, a resistor-capacitance (RC) lowpass filter, and a Bluetooth module. The sensing unit and Bluetooth circuit are placed inside the mask's interlayer for real-time oxygen concentration monitoring. The Bluetooth module wirelessly transmits oxygen sensing information to an external device, allowing continuous tracking of respiratory health. A wireless receiving module with a light-emitting diode (LED) is used to confirm successful signal transmission. When there is no signal transmission, the LED remains on. However, as the lung oxygenation level decreases, the piezoelectric output signal increases and reaches the threshold, triggering the Bluetooth module to send a signal to the receiver, which turns off the LED. This function makes the mask useful for alerting users or healthcare providers about oxygen deficiency in real-time.

Fig. 15(e) illustrates how exhaling oxygen concentration changes before and after exercise to simulate lung oxygenation level variations. After exercise, metabolism accelerates, increasing oxygen consumption and reducing exhaled oxygen concentration, a phenomenon known as excess post-exercise oxygen consumption (EPOC). The sensor detects these changes by measuring output voltage variations before and after physical activity. For Subject 1, before exercise, the heart rate was 100 bpm, and the exhaled oxygen concentration was 16%. After running at approximately 15.3 km h^{-1} for 3 min, the heart rate increased to 165 bpm, and the exhaled oxygen concentration decreased to 15%. The sensor's output voltage dropped from 0.139 V to 0.107 V, confirming the sensor's ability to detect physiological oxygen changes accurately. For Subject 2, before exercise, the heart rate was 74 bpm, and the exhaled oxygen concentration was 16%. After running at approximately 12.8 km h^{-1} for 3 min, the heart rate increased to 144 bpm, and the exhaled oxygen concentration dropped to 15%. The sensor's output voltage decreased from 0.195 to 0.166 V, further demonstrating the sensitivity and accuracy of the sensing unit in tracking small variations in exhaled oxygen levels. These results confirm that the oxygen-sensing unit has high sensitivity and is capable of detecting small changes in exhaled oxygen levels, meeting the requirements for real-time respiratory health monitoring and exercise physiology studies. The high sensitivity and accuracy of the oxygen-sensing mechanism make this mask a promising tool for early detection of respiratory conditions, continuous patient monitoring, and remote healthcare applications.

3.8. Multiple gas sensing

There is a growing demand for more accessible and less invasive approaches to early disease identification, as conventional methods like blood tests can be invasive, expensive, and
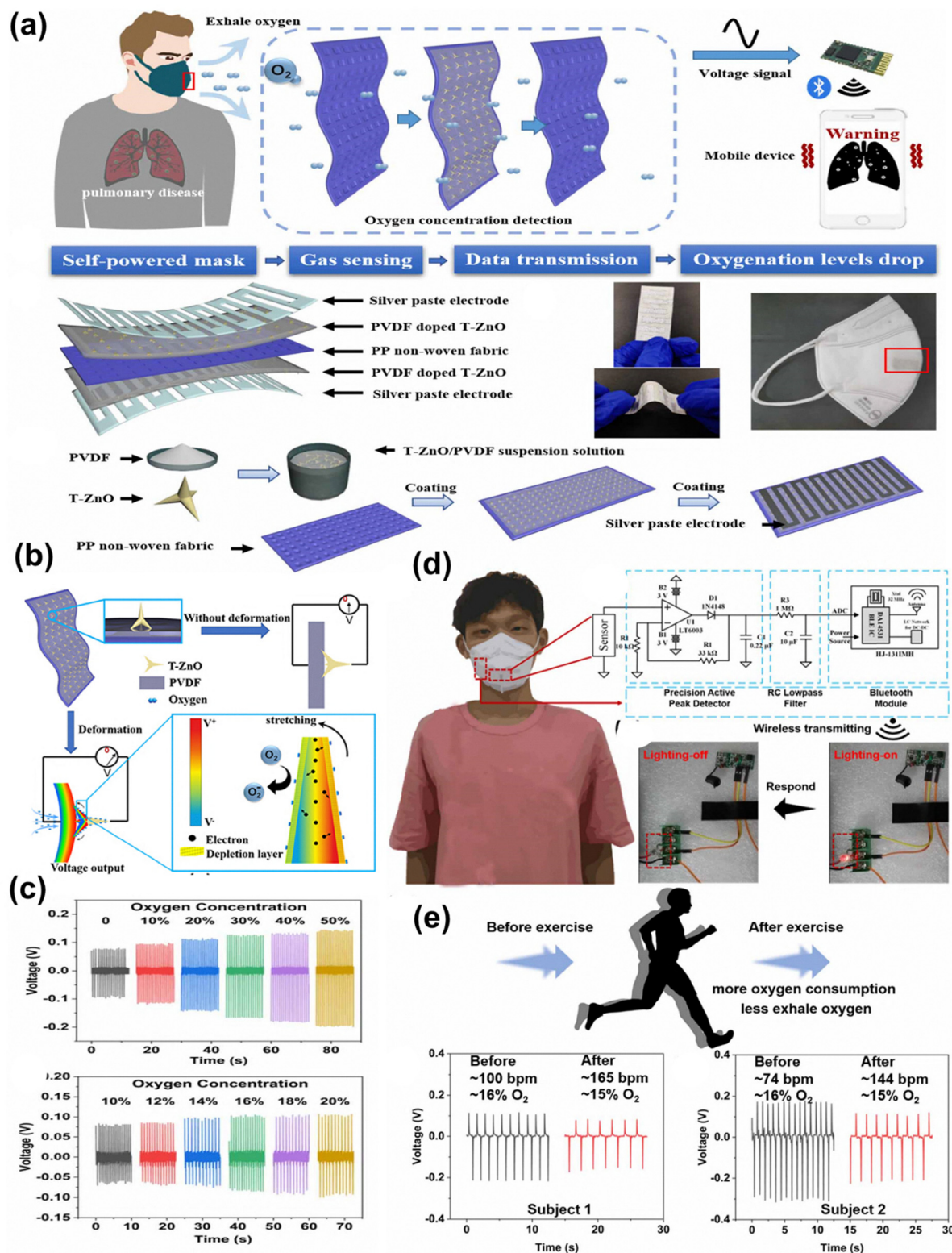
Fig. 15 (a) Schematic of the self-powered exhaling-oxygen-sensing mask and its fabrication process. (b) Working mechanism of the piezoelectric gas sensor under deformation. (c) Sensor response to different oxygen concentrations. (d) Practical application of the mask with wireless data transmission and LED response. (e) Sensor validation before and after exercise for two subjects. Reproduced with permission,[63] Copyright © 2022 IOP Publishing Ltd.

necessitate skilled personnel. Breath analysis offers a non-invasive, real-time diagnostic approach for detecting VOCs

and gas biomarkers linked to diseases like fatty liver (ethanol), airway inflammation (NO_x), diabetes (acetone), liver cirrhosis

(methane), and asthma (CO). Existing breath analyzers, however, are hampered by their high cost, complexity, dependence on external power, and stringent material specifications. Fu and colleagues have introduced a self-powered breath analyzer. This fabricated device combines piezoelectric energy harvesting with gas detection, enabling rapid and non-invasive diagnostic pursuits.[64] A self-powered breath analyzer utilizing a PANI/PVDF piezo-gas-sensing array is presented. This device leverages the synergistic effects of PANI and PVDF for sensitive gas detection and autonomous power generation. The PANI component provides a high surface area and tunable conductivity for efficient gas adsorption and interaction, while the PVDF element, possessing piezoelectric properties, converts mechanical strain induced by gas adsorption into electrical energy. The array architecture further enhances the device's selectivity and sensitivity by providing multiple sensing elements with varying PANI doping levels and PVDF film thicknesses. Preliminary results demonstrate the feasibility of detecting ethanol, acetone, and ammonia, common biomarkers in breath, at relevant concentrations, with the self-generated voltage signal directly correlating with the gas concentration. This self-powered breath analyzer facilitates non-invasive diagnostics and point-of-care applications through continuous, real-time health monitoring without external power.

Fig. 16(a) illustrates the working mechanism of the self-powered breath analyzer, where exhaled breath deforms the PANI/PVDF piezoelectric bellows, generating an electrical signal that is amplified and analyzed. The signal's amplitude varies based on detected gases, enabling breath analysis. Fig. 16(b) displays the un-rolled PANI/PVDF film and the fabricated

bellows, showcasing the device's structure. The fabrication process of the self-powered breath analyzer device involves multiple steps (shown in Fig. 16(c)): at first, copper foil is covered with photoresist using photolithography followed by wet-etching in aqueous sodium persulfate (0.5 mol L^{-1}) for 2 min; after that, it is immersed into a developer for 30 s to remove the residual photoresist. In the second step, to pattern Cu electrodes, electrochemical polymerization of PANI with different dopants (sodium sulfate, sodium dodecylbenzene sulfonate, sodium oxalate, camphorsulfonic acid, and nitric acid) is performed for selective gas sensing. Further, the PVDF gel is spin-coated on PANI electrodes to obtain PVDF/PANI electrodes. Electrode piezoelectricity is enhanced by high-voltage polarization (20 kV mm^{-1} at 80 °C for 30 min). A 100-nm Cu counter electrode is deposited on the back of the PVDF film, and the device is shaped into a bellows-like structure using extrusion molding, improving its mechanical flexibility and energy conversion efficiency. The fabricated device consists of five individual PANI electrodes, each independently connectable to an external circuit for electrical measurements. One can observe that there are five twist-patterned PANI electrodes in a single device, and each PANI derivative is doped with different dopant sources. The sensing units are designated PANI(SS), PANI(SDS), PANI(SO), PANI(CA), and PANI(NA), corresponding to doping with sodium sulphate, sodium dodecylbenzene sulfonate, sodium oxalate, camphorsulfonic acid, and nitric acid, respectively The twist-patterned PANI electrodes enhance durability and stability during high-frequency vibrations caused by exhaled breath. The fabrication process involves photolithography to etch Cu foil into a twist pattern, followed by electrochemical
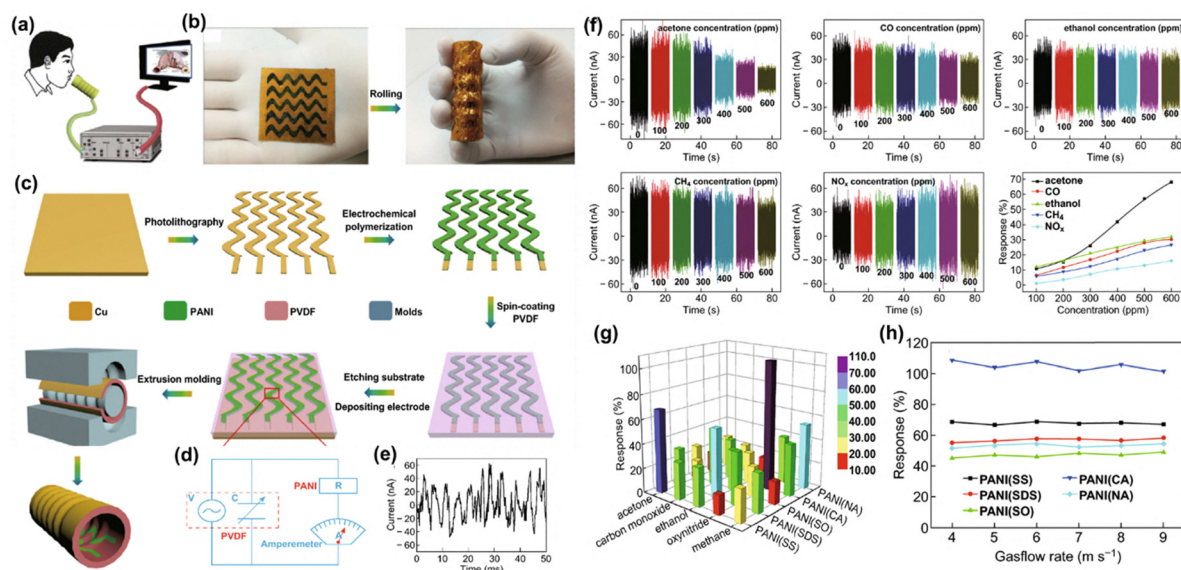

Fig. 16 Structure and fabrication of the device. (a) Proposed concept. (b) Photographs of un-rolled PANI/PVDF film and as-fabricated bellows. (c) Fabrication process of the device. (d) Lumped parameter equivalent circuit model of the device. (e) A few cycles of the output current. (f) Performances of the PANI(SS) sensing unit and the output current of PANI(SS) in response to acetone, CO, ethanol, CH_4, and NO_x with concentrations ranging from 0 to 600 ppm and the relationship between the response and gas concentration. (g) The response of the five sensing units to 600 ppm gases. (h) The relationship of the five sensing units between responses and gas flow rates. Reproduced with permission,[64] Copyright Creative Commons CC BY license © 2018 Springer Nature.

polymerization to deposit five distinct PANI derivatives. A PANI/PVDF film is then created *via* spin-coating the PVDF gel onto the electrodes, and the final bellows structure is formed through extrusion molding.

The operational mechanism leverages the synergistic interaction of PVDF's piezoelectricity and PANI's gas adsorption. In this setup, the deformation from breathing into PVDF generates an alternating electrical signal. At the same time, different gases affect the electrical resistance of PANI, thereby modifying the output signal (as shown in Fig. 16(d and e)). Each variant of PANI interacts distinctly with specific gases, enabling the detection of acetone, ethanol, CO, NO_x, and methane. The device's equivalent circuit comprises a voltage source (V) representing the PVDF piezoelectric potential, a capacitance (C) denoting its intrinsic capacitance, and a resistance (R) defining the PANI gas-sensitive layer. The interplay of these elements determines the resulting AC electrical signal, which serves as the output of the sensor. This signal changes in response to both the intensity of the exhaled breath and the gas concentrations, categorizing it as a dual-function system that performs simultaneously as a self-sustaining energy harvester and a gas sensor.

The experimental results confirm that the analyzer exhibits stable, repeatable responses for gas concentrations ranging from 0 to 600 ppm, with high selectivity and rapid response/recovery times. The bellows configuration enhances mechanical stability, allowing long-term usage without performance degradation. Finally, real-world testing shows its ability to detect ethanol in exhaled breath, mimicking a fatty liver diagnostic application, where the output signal varies proportionally with the concentration of ethanol after alcohol consumption. This study presents a new wearable healthcare monitor that utilizes nanomaterial gas sensors and self-powered energy harvesting for continuous, real-time, and affordable breath analysis in medical diagnostics. Fig. 16(f) illustrates the sensing performance of the PANI(SS) electrode under different gas concentrations ranging from 0 to 600 ppm. The output current response of the PANI(SS) unit is recorded for five different gases: acetone, carbon monoxide (CO), ethanol, oxynitride (NO_x), and methane (CH_4). Fig. 16(f) displays the real-time current output changes for each gas, revealing a distinct trend—acetone, CO, ethanol, and CH_4 cause a decrease in output current with increasing concentration, while NO_x causes an increase. This behavior is attributed to the interaction of gas molecules with the PANI structure, influencing charge transfer and resistance changes. The calculated gas response R (%) as a function of concentration shows a nonlinear trend where response values increase with concentration. Among the tested gases, acetone exhibits the highest response ($\sim 68.2\%$ at 600 ppm), followed by ethanol (31.6%), CH_4 (26.4%), CO (30.3%), and NO_x (15.8%), confirming the high selectivity of PANI(SS) for acetone detection.

The comparative analysis of the gas response percentages of the five PANI-based sensing units at a 600-ppm concentration of their respective target gases is presented in Fig. 16(g). Among them, PANI(CA) exhibits the highest response ($\sim 105.1\%$) to NO_x, indicating exceptional sensitivity toward nitrogen oxides.

The PANI(SS) unit, designed for acetone detection, shows a significant response of $\sim 68.2\%$, followed by PANI(SDS) for ethanol ($\sim 56.9\%$), PANI(NA) for CH_4 ($\sim 53.5\%$), and PANI(SO) for CO ($\sim 47.1\%$). These results confirm that the different PANI derivatives selectively respond to specific gases due to variations in dopant-induced molecular structures, which influence charge transfer and resistance changes. The high selectivity and distinguishable response values among the different sensing units demonstrate the multi-gas detection capability of the breath analyzer, making it effective for real-time monitoring of multiple biomarkers in exhaled breath. Fig. 16(h) examines the influence of gas flow rate (ranging from 4 to 9 m s^{-1}) on the response of all five sensing units. Despite variations in output current, the calculated response remains constant across different flow rates, indicating that the sensor response is independent of airflow rate. The breath analyzer's robustness ensures stable and accurate gas detection, even with varying exhalation force, making it ideal for practical breath analysis.

4. Performance comparison of materials for self-powered breath analyzers

The heatmap presented in this study provides a comparative analysis of key materials used in self-powered breath analyzers, evaluating their performance across four critical parameters: sensitivity, response time, durability, and wearability (presented in Fig. 17). Sensitivity, a crucial factor for gas detection, is observed to be the highest in MXene and ZnO, making them ideal candidates for highly responsive breath sensors. These materials exhibit strong interaction with gas molecules, ensuring precise detection of biomarkers related to respiratory diseases. Graphene-based composites demonstrate a balanced performance across multiple categories, particularly excelling in durability and wearability, which is essential for the development of flexible and wearable sensors integrated into smart textiles or face masks.

In contrast, PVDF-based materials show exceptional wearability and high-power generation efficiency due to their piezoelectric properties, making them suitable for self-powered respiratory monitoring systems. Silicone-based materials, while exhibiting lower sensitivity, provide the highest wearability and comfort, making them ideal for long-term continuous monitoring applications. Response time, another critical factor for real-time breath analysis, is significantly lower in MXene and ZnO-based materials, indicating their rapid detection capabilities, whereas silicone and polymer-based sensors tend to have slightly slower reaction times. The heatmap visualization highlights these performance differences, aiding in the strategic selection of materials based on specific biomedical application needs. Overall, the findings from this analysis underscore the importance of material selection in optimizing breath analyzer performance, ensuring real-time, accurate, and wearable respiratory monitoring solutions.

5. Challenges and future improvements

One of the key challenges facing TENG-based gas sensors is ensuring environmental stability, as their performance can be significantly influenced by external factors such as humidity and temperature fluctuations. As mentioned previously by Mohamadbeigi *et al.*,[25] variations in environmental conditions can change the triboelectric output and the gas sensing response, leading to inconsistencies in sensor performance over time. To address this, future improvements have to focus on optimizing the materials used for both energy harvesting and gas detection, developing surfaces that are less sensitive to moisture and temperature changes (Fig. 18). Enhancing environmental stability will be critical for enabling the reliable, long-term operation of TENG-based sensors in real-world healthcare and wearable applications.

TENG-based gas sensors offer significant advantages, including being lightweight, portable, and self-powered, making them suitable for applications in environmental monitoring, food safety, and personal health.[65] Future sensors will need to enable real-time, dynamic monitoring and transmission of data to smartphones or cloud servers for remote analysis and feedback. This interconnected system of people, devices, and data increases demands on signal acquisition, transmission, and device wearability. TENG-based sensors provide a robust platform to overcome power limitations and support wearable, continuous gas sensing.

Large-scale manufacturing of TENGs and PENGs faces several challenges limiting their commercial deployment, such as maintaining uniformity and performance, particularly due to material incompatibility between optimal piezoelectric and triboelectric components.[66,67] Designing structures for efficient energy harvesting from multiple mechanical modes, such as compression, strain, and contact-separation, requires advanced engineering because poor interface integration often causes mechanical losses and electrical mismatches. Another challenge is the degradation of the devices due to environmental conditions like humidity and temperature.[68] Moreover, fabrication methods achieve high efficiency on the lab scale, while for large-scale production, they may have low precision depending on the fabrication techniques.[69] Overcoming these challenges demands progress in materials science, device architecture, scalable fabrication, and system integration to enable consistent, high-quality nanogenerator production.

TENG-based gas sensors also demonstrate enhanced sensitivity and selectivity, owing to the unique interaction between the electrical output generated by the TENG and the gas adsorption processes occurring on the sensor surface, as indicated by Luo *et al.*[70] This interaction results in faster response times and significantly lower LOD compared to conventional sensors. Moreover, by carefully tailoring the sensing materials, such as utilizing WO_3, ZnO, and MXene/CuO composites for different VOCs such as ethanol, acetone, and ammonia monitoring, these sensors achieve high selectivity toward specific target gases.[71–73] This material customization not only improves detection accuracy but also broadens the application scope of TENG-based sensors for precise and reliable health diagnostics.[74–76]

A major advantage of TENG-based gas sensors is their ability to operate efficiently at RT, unlike conventional gas sensors that often require high operating temperatures to achieve adequate sensitivity.[76,77] This room temperature functionality significantly reduces overall energy consumption, making the sensors more suitable for continuous, low-power operation.[49,78] Additionally, it enhances their practicality for real-time health diagnostics, particularly in wearable and portable applications where minimal heat generation and immediate responsiveness
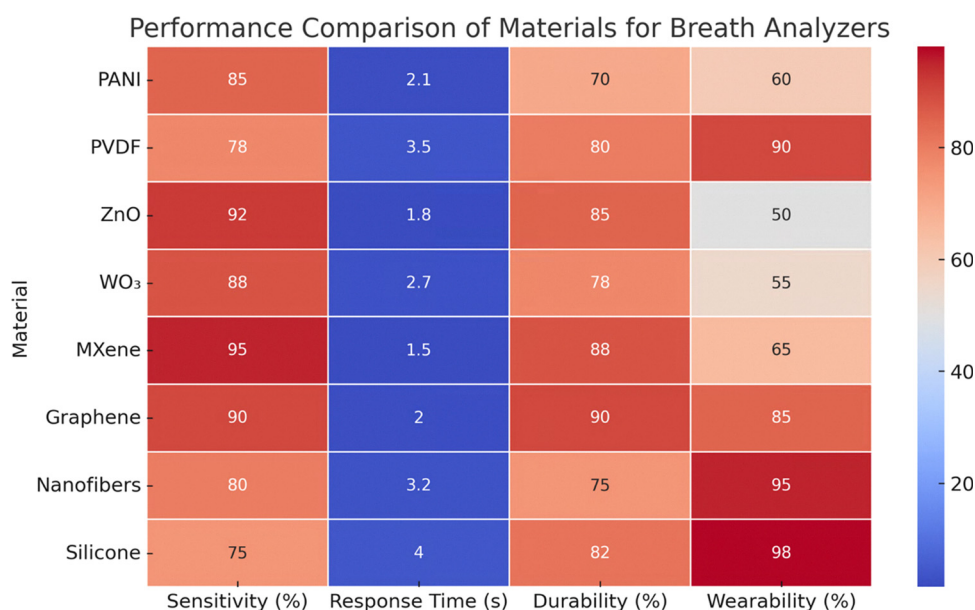
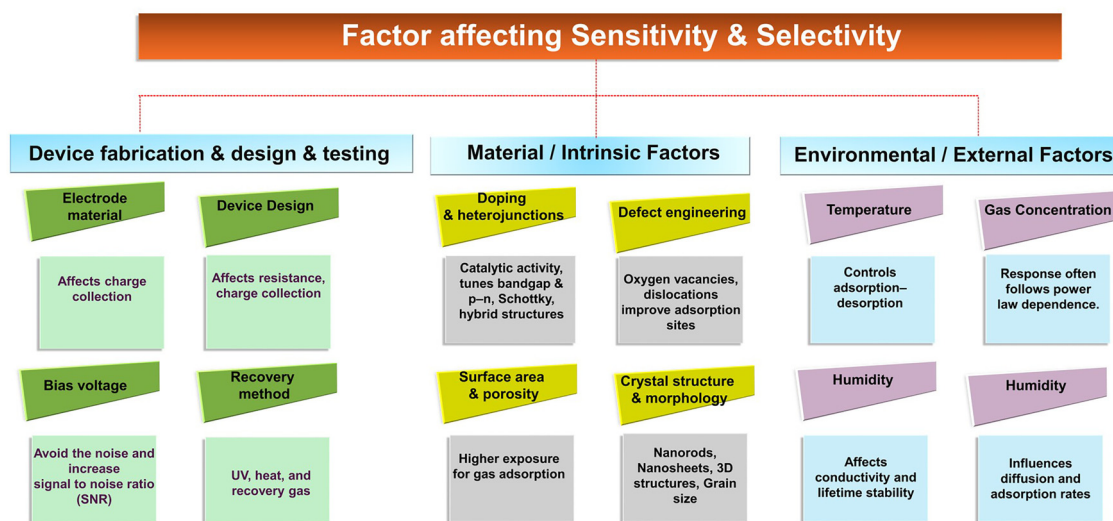Fig. 17 Performance comparison of materials for breath analyzers.

Fig. 18 Factors affecting the sensitivity and selectivity of sensors.

are crucial.[24] By eliminating the need for external heating elements, TENG-based sensors offer a safer, more energy-efficient solution for non-invasive, on-the-go medical monitoring.[58]

Long-term durability is a critical factor in the commercial viability of TENG-based gas sensors, especially for applications in continuous health monitoring.[65] Prolonged exposure to real-world conditions, such as mechanical wear, temperature shifts, and humidity, can compromise sensor performance over time. To ensure consistent functionality and operational stability, future research must prioritize the development of robust sensing materials along with effective encapsulation strategies that protect the sensor without hindering sensitivity.

Additionally, the use of hybrid nanogenerator systems, combining TENGs with piezoelectric or thermoelectric elements, offers a promising path to enhance energy efficiency, enabling more reliable and self-sustained operation in diverse environments. Moving forward, the development of TENG-based sensors will also depend on their ability to perform complex diagnostic tasks, such as detecting multiple gas biomarkers simultaneously.[79] Developing multi-gas sensing platforms integrated with miniaturized electronics can provide a more comprehensive analysis of health conditions through breath analysis. Furthermore, coupling these sensors with IoT networks and AI-driven analytics facilitates real-time data analysis, predictive diagnostics, and personalized health insights. Such integration not only improves diagnostic accuracy but also paves the way for intelligent, connected healthcare systems capable of early disease detection and proactive medical intervention.[80,81]

6. Conclusions

The incorporation of self-powered technology into gas sensing systems represents a significant step forward in the direction of non-invasive, real-time, and personalized health monitoring systems. This review has demonstrated the revolutionary potential of self-powered gas sensors, notably in terms of exhaled breath analysis for biomedical diagnostics. Self-powered sensors minimize the need for external power supplies by capturing ambient energy from the human body or the surroundings, thereby allowing the device to be portable, wearable, and inexpensive. These properties are crucial in the development of next-generation diagnostic systems for point-of-care applications.

Machine learning algorithms, such as logistic regression, K-nearest neighbor (KNN), random forest (RF), linear regression, linear discriminant analysis (LDA), decision tree (DT), naive Bayes (NB), artificial neural network (ANN), and support vector machine (SVM), have emerged as a powerful tool for VOC detection owing to their strong pattern recognition capabilities, which allow rapid and accurate identification of target gases even within complex mixed-gas environments. Nonetheless, several challenges persist, including variations in sensor responses, interference from noise, and data imbalance resulting from differences in gas concentrations. Despite these obstacles, continuous model optimization and parameter tuning can substantially improve both the accuracy and efficiency of gas detection systems.

We have explored a variety of energy harvesting techniques, including triboelectric and piezoelectric nanogenerators, that can be effortlessly integrated into gas sensor systems. Material engineering and structural design advancements have considerably enhanced the sensitivity, selectivity, and mechanical adaptability of these sensors, making them more suitable for complicated biological environments. Patches, facemasks, and implantable modules are examples of wearable diagnostic devices that are becoming smaller and more user-friendly, enabling convenient and continuous health monitoring.

However, significant challenges have to be addressed before these technologies may reach clinical and commercial viability. These issues include enhancing specificity for low-concentration biomarkers, assuring signal stability under changing conditions,

reducing production costs, and achieving reliable data interpretation using AI-assisted analytics. Moving forward, multidisciplinary collaborations between materials science, electronics, data science, and biological engineering are important to do more research in this field. With continuing improvement, self-powered gas sensors have the potential to transform healthcare systems by offering continuous, real-time, and specialized disease diagnosis in both clinical settings and daily life.

Conflicts of interest

The authors declare no conflict of interest.

Data availability

No new data were generated or analyzed in this study. Sources of original data are cited appropriately in the figure captions.

Acknowledgements

References

1 P. Singh, *et al.*, Recent Progress on Perovskite Materials for VOC Gas Sensing, *Langmuir*, 2024, **40**(42), 21931–21956.

2 G. V. Silva, *et al.*, Low-VOC Emission Label Proposal for Facemask Safety Based on Respiratory and Skin Health Criteria, *Environments*, 2023, **10**, 10.

3 K. Liu, *et al.*, Rational Design and Application of Breath Sensors for Healthcare Monitoring, *ACS Sens.*, 2025, **10**(1), 15–32.

4 K. Swargiary, *et al.*, Highly sensitive and real-time detection of acetone biomarker for diabetes using a ZnO-coated optical fiber sensor, *Biosens. Bioelectron.*, 2025, **271**, 117061.

5 H. Kafeenah and M. O. Eze, Trends in volatile organic compound-based metabolomics for biomarker discovery, *Microchem. J.*, 2025, **213**, 113700.

6 H. Lee, *et al.*, A graphene-based electrochemical device with thermoresponsive microneedles for diabetes monitoring and therapy, *Nat. Nanotechnol.*, 2016, **11**(6), 566–572.

7 H. Zhao, *et al.*, Proton-Conductive Gas Sensor: a New Way to Realize Highly Selective Ammonia Detection for Analysis of Exhaled Human Breath, *ACS Sens.*, 2020, **5**(2), 346–352.

8 M. A. Belal, *et al.*, Advances in gas sensors using screen printing, *J. Mater. Chem. A*, 2025, **13**(8), 5447–5497.

9 P. C. Tagbo, *et al.*, Fabrication of flexible MoS$_2$ sensors for high-performance detection of ethanol vapor at room temperature., *Sens. Actuators, A*, 2025, **389**, 116531.

10 V. Suthat Na Ayutaya, *et al.*, Urinary cancer detection by the target urine volatile organic compounds biosensor platform, *Sci. Rep.*, 2024, **14**(1), 3551.

11 B. Vadhwana, *et al.*, Salivary Volatile Organic Compound Analysis: An Optimised Methodology and Longitudinal Assessment Using Direct Injection Mass Spectrometry, *Appl. Sci.*, 2023, **13**(7), 4084.

12 X. B. Li, *et al.*, Identification of volatile organic compounds in muscle tissues of different species based on Headspace-Gas-Chromatography Ion-Mobility spectrometry, *Leg Med.*, 2022, **59**, 102132.

13 P. Mochalski, *et al.*, Identification of Key Volatile Organic Compounds Released by Gastric Tissues as Potential Non-Invasive Biomarkers for Gastric Cancer, *Diagnostics*, 2023, **13**(3), 335.

14 S. Y. Ruan, *et al.*, Inhaled nitric oxide therapy and risk of renal dysfunction: a systematic review and meta-analysis of randomized trials, *Crit. Care*, 2015, **19**(1), 137.

15 A. Tricoli and G. Neri, Miniaturized Bio-and Chemical-Sensors for Point-of-Care Monitoring of Chronic Kidney Diseases, *Sensors*, 2018, **18**(4), 942.

16 C. Bayona, *et al.*, Development of an organ-on-chip model for the detection of volatile organic compounds as potential biomarkers of tumour progression, *Biofabrication*, 2024, **16**(4), 045002.

17 S. T. Wang, G. Gerlach and J. Körner, A study of smart hydrogels as sensing elements in gaseous environment for VOC detection, *Polymer*, 2023, **278**, 126009.

18 M. Khatib and H. Haick, Sensors for Volatile Organic Compounds, *ACS Nano*, 2022, **16**(5), 7080–7115.

19 S. S. Chen, *et al.*, Fabrication of Fe2O3@SnO2 nanofiber gas sensors to identify VOCs in mixed-gas environments using dynamic modulation and the machine learning algorithm, *Chem. Eng. J.*, 2025, **519**, 165402.

20 Anju, L. K. Saini and M. Pandey, Quantum chemical analysis of porphyrin-based sensors: Adsorption and sensing capabilities of pure, protonated, and metallic porphyrins insights into volatile organic compounds (VOCs), *Mater. Today Commun.*, 2024, **41**, 110989.

21 D. S. Li, *et al.*, Virtual sensor array based on MXene for selective detections of VOCs, *Sens. Actuators, B*, 2021, **331**, 129414.

22 S. A. Behera, *et al.*, Self-Powered Wind Flow Monitoring Unit Using Lead-Free Composites-Based Triboelectric Nanogenerator. Acs Applied Energy, *Materials*, 2025, **8**(10), 6688–6698.

23 S. Hajra, *et al.*, Self-Powered Fire Safety Indicator Based on Fabric-Based Triboelectric Nanogenerator, *Energy Technol.*, 2025, 2402488.

24 S. Lee, H.-J. Ko and J. Kim, Self-powered gas sensor based on triboelectric nanogenerators (TENG): a comparative review of sensing mechanisms, *Micro Nano Syst. Lett.*, 2025, **13**, 1–10.

25 N. Mohamadbeigi, *et al.*, Self-powered triboelectric nanogenerator sensor for detecting humidity level and monitoring ethanol variation in a simulated exhalation environment, *Sci. Rep.*, 2024, **14**(1), 1562.

26 I. K. Oh, *et al.*, Synthesis of a Hybrid Nanostructure of ZnO-Decorated MoS(2) by Atomic Layer Deposition, *ACS Nano*, 2020, **14**(2), 1757–1769.

27 M. A. Belal, *et al.*, Functionalized MWCNTs@ZnO nanocomposites *via* spray printing for NO gas sensing, *J. Mater. Sci.: Mater. Electron.*, 2025, **36**, 750.

28 T. T. Tung, *et al.*, Graphene and metal organic frameworks (MOFs) hybridization for tunable chemoresistive sensors for detection of volatile organic compounds (VOCs) biomarkers, *Carbon*, 2020, **159**, 333–344.

29 Z. F. Yin, *et al.*, Wearable respiratory sensors for health monitoring, *Npg Asia Mater.*, 2024, **16**, 8.

30 S. M. Ledford and L. K. Meredith, Volatile Organic Compound Metabolism on Early Earth, *J. Mol. Evol.*, 2024, **92**(5), 605–617.

31 T. J. Maginga, *et al.*, Design and implementation of IoT sensors for nonvisual symptoms detection on maize inoculated with Exserohilum turcicum, *Smart Agric. Technol.*, 2023, **5**, 100260.

32 S. Honda, *et al.*, A wearable, flexible sensor for real-time, home monitoring of sleep apnea, *iScience*, 2022, **25**(4), 104163.

33 M. R. Chen, *et al.*, AI-Driven Wearable Mask-Inspired Self-Healing Sensor Array for Detection and Identification of Volatile Organic Compounds, *Adv. Funct. Mater.*, 2024, **34**, 2309732.

34 R. J. Rath, *et al.*, Chemiresistive Sensor Arrays for Gas/Volatile Organic Compounds Monitoring: A Review, *Adv. Eng. Mater.*, 2023, **25**(3), 2200830.

35 L. Lu, *et al.*, Noncontact 3D gesture recognition enabled VR human-machine interface *via* electret-nanofiber-based triboelectric sensor, *Nano Res.*, 2025, DOI: **10.26599/NR.2025. 94907924**.

36 B. S. Zhang, *et al.*, Recent advances in nature inspired triboelectric nanogenerators for self-powered systems, *Int. J. Extreme Manuf.*, 2024, **6**, 062003.

37 G. Khandelwal, S. Deswal and R. Dahiya, Triboelectric Nanogenerators as Power Sources for Chemical Sensors and Biosensors, *ACS Omega*, 2022, **7**(49), 44573–44590.

38 A. Babu, *et al.*, Functionalized MIL-125(Ti)-based high-performance triboelectric nanogenerators for hygiene monitoring, *Mater. Adv.*, 2025, **6**(14), 4725–4737.

39 S. Atkare, C. S. Rout and S. Jagtap, Perspectives of 2D MXene-based materials for self-powered smart gas sensors, *Mater. Adv.*, 2024, **5**(4), 1440–1453.

40 W. Kwak, *et al.*, Advances in triboelectric nanogenerators for self-powered wearable respiratory monitoring., *FlexMat*, 2024, **1**(1), 5–22.

41 S. Anbalagan, *et al.*, Progress and recent advances in self-powered gas sensing based on triboelectric and piezoelectric nanogenerators, *Chem. Eng. J.*, 2024, **497**, 154740.

42 W. X. Li, *et al.*, Piezoelectric composites for gas sensing: evolution of sensing and transduction designs, *J. Mater. Chem. C*, 2025, **13**(27), 13582–13606.

43 Z. Wen, *et al.*, Blow-driven triboelectric nanogenerator as an active alcohol breath analyzer, *Nano Energy*, 2015, **16**, 38–46.

44 B. H. Liu, *et al.*, Novel chitosan/ZnO bilayer film with enhanced humidity-tolerant property: Endowing triboelectric nanogenerator with acetone analysis capability, *Nano Energy*, 2020, **78**, 105256.

45 B. Liu, *et al.*, Simultaneous Biomechanical and Biochemical Monitoring for Self-Powered Breath Analysis, *ACS Appl. Mater. Interfaces*, 2022, **14**(5), 7301–7310.

46 S. Wang, *et al.*, A facile respiration-driven triboelectric nanogenerator for multifunctional respiratory monitoring, *Nano Energy*, 2019, **58**, 312–321.

47 L. Liu, *et al.*, Highly sensitive and chemically stable NH(3) sensors based on an organic acid-sensitized cross-linked hydrogel for exhaled breath analysis, *Biosens. Bioelectron.*, 2021, **191**, 113459.

48 L. C. Liu, *et al.*, Humidity-activated ammonia sensor with excellent selectivity for exhaled breath analysis, *Sens. Actuators, B*, 2021, **334**, 129625.

49 S. Veeralingam and S. Badhulika, Ti@MoS$_2$ incorporated Polypropylene/Nylon fabric-based porous, breathable triboelectric nanogenerator as respiration sensor and ammonia gas sensor applications., *Sens. Actuators, B*, 2023, **380**, 133346.

50 S. Sardana and A. Mahajan, Edge-Site-Enriched Ti$_3$C$_2$T$_x$ MXene/MoS2 Nanosheet Heterostructures for Self-Powered Breath and Environmental Monitoring, *ACS Appl. Nano Mater.*, 2022, **6**(1), 469–481.

51 S. Wang, *et al.*, Ultrasensitive flexible self-powered ammonia sensor based on triboelectric nanogenerator at room temperature, *Nano Energy*, 2018, **51**, 231–240.

52 Y. Su, *et al.*, Alveolus-Inspired Active Membrane Sensors for Self-Powered Wearable Chemical Sensing and Breath Analysis, *ACS Nano*, 2020, **14**(5), 6067–6075.

53 D. Wang, *et al.*, Multifunctional poly(vinyl alcohol)/Ag nanofibers-based triboelectric nanogenerator for self-powered MXene/tungsten oxide nanohybrid NO2 gas sensor, *Nano Energy*, 2021, **89**, 106410.

54 Y. Su, *et al.*, Self-powered room temperature NO2 detection driven by triboelectric nanogenerator under UV illumination, *Nano Energy*, 2018, **47**, 316–324.

55 S. Das, *et al.*, Self-Powered cobalt nanocluster decorated flexible graphene based Tribo-Sensors for respiratory diagnosis of critical asthma patient, *Chem. Eng. J.*, 2024, **492**, 152319.

56 L. Y. Wang, J. Song and C. Y. Yu, Recent advances in formaldehyde sensors: a review, *J. Iran. Chem. Soc.*, 2024, **21**(6), 1495–1507.

57 D. Y. Wang, *et al.*, Multifunctional respiration-driven triboelectric nanogenerator for self-powered detection of formaldehyde in exhaled gas and respiratory behavior, *Nano Energy*, 2022, **102**, 107711.

58 C. Y. Chang, Y. H. Cheng and C. Y. Ho, Surface engineering of a triboelectric nanogenerator for room temperature high-performance self-powered formaldehyde sensors, *J. Mater. Chem. A*, 2022, **10**(42), 22373–22389.

59 F. I. Ali, *et al.*, Hydrogen sulfide (H 2 S) gas sensor: A review, *IEEE Sens. J.*, 2018, **19**(7), 2394–2407.

60 W. Huang, *et al.*, Design of stretchable and self-powered sensing device for portable and remote trace biomarkers detection, *Nat. Commun.*, 2023, **14**(1), 5221.

61 B. H. Liu, *et al.*, Lever-inspired triboelectric respiration sensor for respiratory behavioral assessment and exhaled

hydrogen sulfide detection, *Chem. Eng. J.*, 2023, **471**, 144795.

62 L. Huang, *et al.*, Noninvasive Diagnosis of Gastric Cancer Based on Breath Analysis with a Tubular Surface-Enhanced Raman Scattering Sensor, *ACS Sens.*, 2022, **7**(5), 1439–1450.

63 Y. X. Lin, *et al.*, A wearable exhaling-oxygen-sensing mask based on piezoelectric/gas-sensing coupling effect for real-time monitoring and uploading lung disease information, *J. Phys. D: Appl. Phys.*, 2022, **55**(22), 224001.

64 Y. Fu, *et al.*, A Self-Powered Breath Analyzer Based on PANI/PVDF Piezo-Gas-Sensing Arrays for Potential Diagnostics Application, *Nanomicro Lett.*, 2018, **10**(4), 76.

65 P. Lu, *et al.*, Advanced application of triboelectric nanogenerators in gas sensing, *Nano Energy*, 2024, **126**, 109672.

66 R. Walden, *et al.*, Opportunities and Challenges in Triboelectric Nanogenerator (TENG) based Sustainable Energy Generation Technologies: A Mini-Review, *Chem. Eng. J. Adv.*, 2022, **9**, 100237.

67 Z. Turar, *et al.*, Advances in Porous Structure Design for Enhanced Piezoelectric and Triboelectric Nanogenerators: A Comprehensive Review, *Glob. Chall.*, 2025, **9**(1), 2400224.

68 D. M. Tiruneh and H. Ryu, Recent advances in nanogenerators for wearable electronic devices, *APL Electron. Dev.*, 2025, **1**, 011501.

69 A. Kumar, *et al.*, Recent progress in nanocomposite-oriented triboelectric and piezoelectric energy generators: An overview, *Nano-Struct. Nano-Objects*, 2023, **36**, 101046.

70 Y. Luo, *et al.*, Highly ammonia-sensitive triboelectric materials enabled by gas-sensing enhancement effect, *Chem. Eng. J.*, 2025, **507**, 160466.

71 L. Piliai, *et al.*, NAP-XPS study of surface chemistry of CO and ethanol sensing with WO_3 nanowires-based gas sensor, *Sens. Actuators, B*, 2023, **397**, 134682.

72 J. Tian, *et al.*, Self-Powered Room-Temperature Ethanol Sensor Based on Brush-Shaped Triboelectric Nanogenerator, *Research*, 2021, 8564780.

73 S. He, *et al.*, $CuO/TiO(2)/MXene$-Based Sensor and SMS-TENG Array Integrated Inspection Robots for Self-Powered Ethanol Detection and Alarm at Room Temperature, *ACS Sens.*, 2024, **9**(3), 1188–1198.

74 B. Liu, *et al.*, A Room Temperature-Operating Acetone Gas Sensor Based on the Triboelectric Effect. ECS Meeting Abstracts, 2020. (28): 2122.

75 D. Y. Wang, *et al.*, Quantitative detection of multi-component chemical gas *via* MXene-based sensor array driven by triboelectric nanogenerators with CNN-GRU model, *Sens. Actuators, B*, 2024, **417**, 136101.

76 X. W. Wang, *et al.*, A room temperature ammonia gas sensor based on cerium oxide/MXene and self-powered by a freestanding-mode triboelectric nanogenerator and its multifunctional monitoring application, *J. Mater. Chem. A*, 2023, **11**(14), 7690–7701.

77 S. He, *et al.*, A self-powered $β$-$Ni(OH)_2$/MXene based ethanol sensor driven by an enhanced triboelectric nanogenerator based on $β$-$Ni(OH)_2$@PVDF at room temperature, *Nano Energy*, 2023, **107**, 108132.

78 D. Zhang, *et al.*, Triboelectric Nanogenerator for Self-Powered Gas Sensing, *Small*, 2024, **20**(51), e2406964.

79 M. Harun-Or-Rashid, S. Mirzaei and N. Nasiri, Nanomaterial Innovations and Machine Learning in Gas Sensing Technologies for Real-Time Health Diagnostics, *ACS Sens.*, 2025, **10**(3), 1620–1640.

80 M. Chen, *et al.*, Triboelectric nanogenerator and artificial intelligence to promote precision medicine for cancer, *Nano Energy*, 2022, **92**, 106783.

81 A. Baburaj, *et al.*, AI-Driven TENGs for Self-Powered Smart Sensors and Intelligent Devices, *Adv. Sci.*, 2025, **12**(20), e2417414.